

Old Dominion University
ODU Digital Commons

CCPO Publications

Center for Coastal Physical Oceanography

1986


The Physics of the Antarctic Circumpolar Current

Worth D. Nowlin

John M. Klinck

Old Dominion University, jklinck@odu.edu

Follow this and additional works at: https://digitalcommons.odu.edu/ccpo_pubs

 Part of the [Climate Commons](#), [Geophysics and Seismology Commons](#), and the [Oceanography Commons](#)

Repository Citation

Nowlin, Worth D. and Klinck, John M., "The Physics of the Antarctic Circumpolar Current" (1986). *CCPO Publications*. 90.
https://digitalcommons.odu.edu/ccpo_pubs/90

Original Publication Citation

Nowlin, W.D., & Klinck, J.M. (1986). The physics of the Antarctic Circumpolar Current. *Reviews of Geophysics*, 24(3), 469-491.

This Article is brought to you for free and open access by the Center for Coastal Physical Oceanography at ODU Digital Commons. It has been accepted for inclusion in CCPO Publications by an authorized administrator of ODU Digital Commons. For more information, please contact digitalcommons@odu.edu.

The Physics of the Antarctic Circumpolar Current

WORTH D. NOWLIN, JR., AND JOHN M. KLINCK

Department of Oceanography, Texas A&M University, College Station

A region of transition of surface water characteristics from subantarctic to antarctic and an associated eastward flowing Antarctic Circumpolar Current (ACC) have long been recognized to exist as a band around Antarctica. In this review we summarize the most important observational and theoretical findings of the past decade regarding the ACC, identify gaps in our knowledge, and recommend studies to address these. The nature of the meridional zonation of the ACC is only now being revealed. The ACC seems to exist as multiple narrow jets imbedded in, or associated with, density fronts (the Subantarctic and Polar fronts) which appear to be circumpolar in extent. These fronts meander, and current rings form from them; lateral frontal shifts of as much as 100 km in 10 days have been observed. The volume transport of the ACC has been estimated many times with disparate results. Recently, yearlong direct measurements in Drake Passage have shown the mean transport to be approximately $134 \times 10^6 \text{ m}^3/\text{s}$, with an uncertainty of not more than 10%. The instantaneous transport can vary from the mean by as much as 20%, with most of the variation associated with changes in the reference flow at 2500 m rather than in the vertical shear. Meridional exchanges of heat across the ACC are known to be important to the heat balance of the abyssal ocean and consequently to global climate. The most likely candidate process for the required poleward heat exchange seems to be mesoscale eddies, though narrow abyssal boundary currents may also be important. Observations from ships, drifters, and satellites reveal surface mean kinetic energy to be at a maximum along the axis of the ACC and eddy kinetic energy to be large mainly in western boundary regions and off the tip of Africa. Eddy variability in the open ocean is consistent with baroclinic instability of the narrow jets. Calculations using data from Drake Passage show that the necessary conditions for baroclinic and barotropic instabilities are met in the ACC. The basic dynamical balance of the ACC is still not well known, although bottom and lateral topography and dynamic instabilities are shown to be important in balancing wind forcing. The ACC is generally conceded to be driven by the wind, but the coupling of wind and thermohaline circulations have not yet been adequately investigated. The mechanism responsible for the multiple cores of the ACC has not been identified in detail. It is suggested that future studies address: (1) the circumpolar structure and temporal behavior of the Subantarctic Front and Polar Front; (2) the general dynamical balance of the ACC and specific mechanisms for creation and maintenance of the major fronts; (3) the representativeness to the entire ACC of the existing estimates of meridional exchanges of heat and other properties, as well as kinematic and dynamic quantities, made in Drake Passage; (4) the variability of the ACC transport in several places and coherence of its variability; (5) the climatology of fields of atmosphere-ocean forcing over the southern ocean; and (6) the possibility of identifying and using simple indices as good indicators of the behavior of the ACC or parts thereof.

CONTENTS

| | |
|---|-----|
| Introduction | 469 |
| Zonation | 471 |
| Zonal transport | 473 |
| Meridional exchanges | 475 |
| Kinematic and dynamical estimates | 478 |
| Circumpolar distribution | 478 |
| Site specific estimates | 480 |
| Theory and models | 483 |
| Basic dynamical problem of the ACC | 483 |
| Simplified dynamical models of the ACC | 483 |
| The ACC as part of a global ocean model | 486 |
| Mesoscale dynamics in the ACC | 487 |
| Summary remarks and suggestions | 488 |

1. INTRODUCTION

A region of transition between surface waters with antarctic and subantarctic characteristics has long been recognized to exist as a band around Antarctica [Meinardus, 1923]. Associated in some manner with this transition, a major eastward flowing surface current has likewise been known. Most early data were derived from ships' logs and from vessels operating in support of the whaling and sealing industries. More recently, national scientific expeditions, such as the *Eltanin* program,

have greatly added to our reconnaissance data, especially with deeper observations. On the basis of the best available station data selected for the *Southern Ocean Atlas* [Gordon and Molinelli, 1982], Gordon *et al.* [1978] described the large-scale relative dynamic topography of the southern ocean. The Antarctic Circumpolar Current (ACC) is clearly visible in their representation of the geostrophic surface current relative to 1000 dbar (Figure 1). The position of the flow is seen to vary considerably in latitude, in large measure owing to geomorphological influences. Even for this coarse representation (1° latitude by 2° longitude) of data collected at different times, multiple paths and apparent differences in width are seen. Gordon *et al.* [1978] also showed that the baroclinicity of the ACC extends throughout the water column, with varying strength in different regions.

The ACC is generally conceded to be driven principally by surface wind stress, though the coupling and relative importance of wind and thermohaline driving has not been adequately investigated. Figure 2 shows the annual mean eastward component of wind stress prepared by S. Patterson (personal communication, 1985) using the climatological surface winds prepared by Han and Lee [1981]. Many models have shown the wind stress to be sufficient to drive the ACC. However, the mechanisms responsible for energy dissipation from the ACC are as yet unclear. Four major mechanisms have been advanced: form drag due to bottom topography [Munk and Palmén, 1951], thermodynamic effects [Fofonoff, 1955],

Copyright 1986 by the American Geophysical Union.

Paper number 6R0315.
8755-1209/86/006R-0315\$15.00

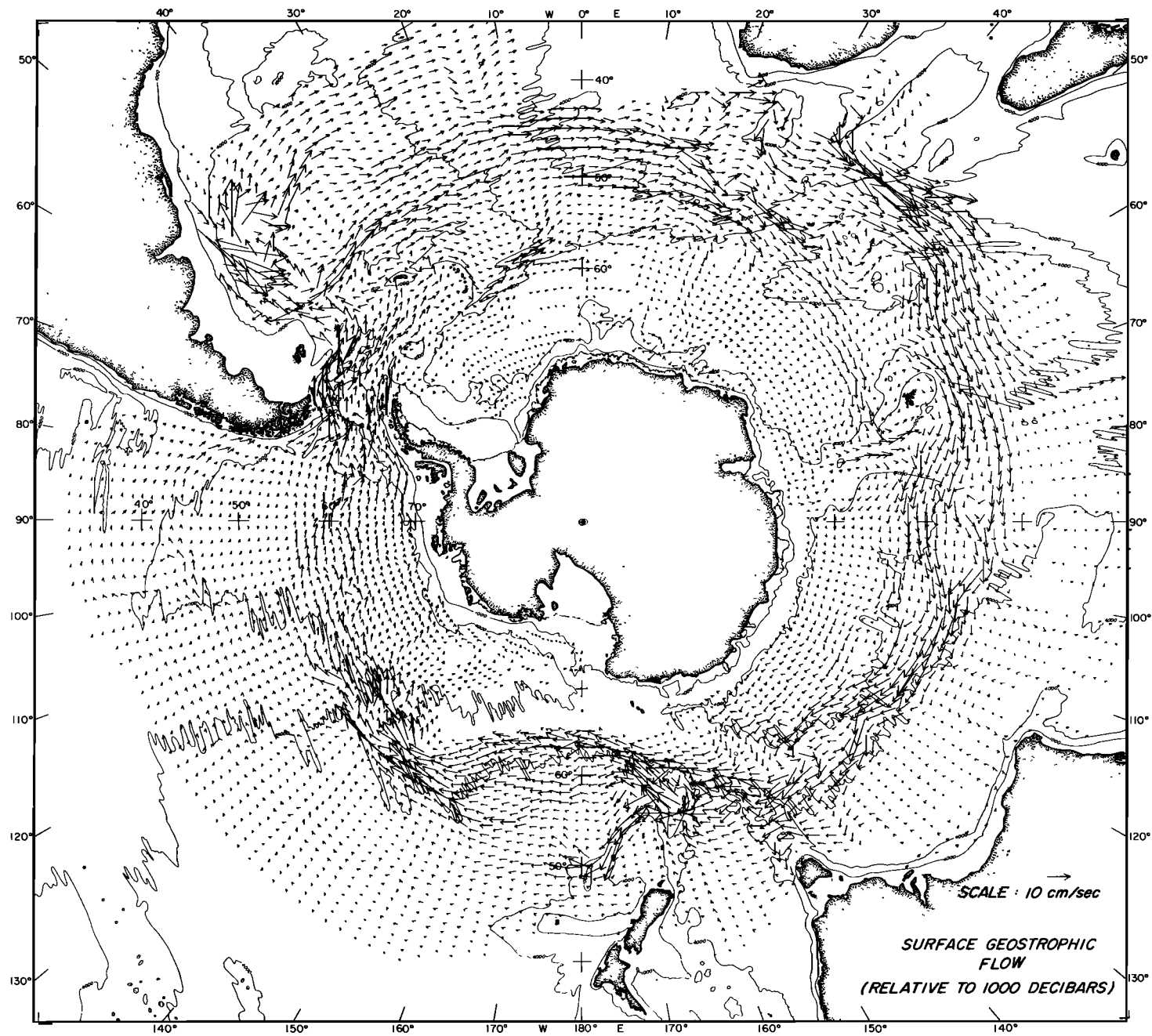


Fig. 1. Geostrophic current at the sea surface relative to 1000 dbar from historical hydrographic data. Current components evaluated from 1° latitude by 2° longitude grid point values [Gordon et al., 1978].

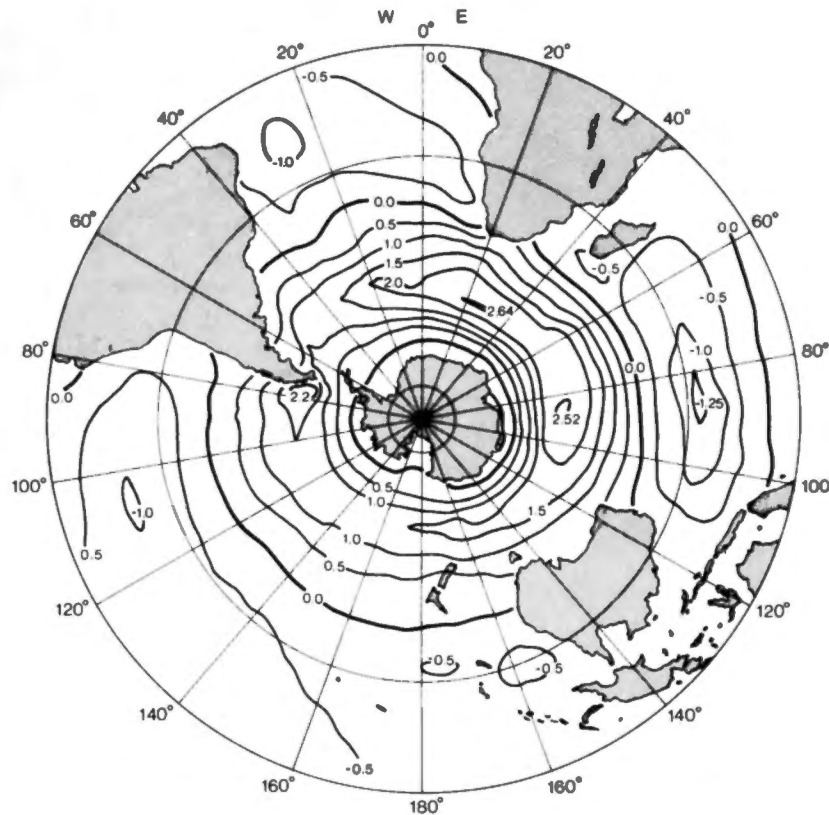


Fig. 2. Annual mean eastward wind stress (units of 0.1 N/m^2) prepared by S. Patterson from climatological surface winds of Han and Lee [1981].

nonzonal dynamics [Stommel, 1957], and water discharged from Antarctica [Barcilon, 1966, 1967]. The overall vorticity balance is still in doubt [Baker, 1982], although a simple Sverdrup balance with dissipative mechanisms of form drag by bottom topography and lateral dissipation in western boundary layers is consistent with existing data.

The southern ocean is a region where atmosphere-ocean exchanges cause strong near-surface modifications and production of water masses which spread throughout the global ocean. A. Gordon (as cited by deSzoeke and Levine [1981]) has estimated the heat transfer from sea to air south of the Polar Front to be $3 \times 10^{14} \text{ W}$. This heat loss must be balanced by poleward oceanic heat flux across the ACC. The traditional concept that this flux is brought about by mean meridional advection of water masses through the predominantly zonal flow of the ACC has been challenged by recent observations which suggest a large role for eddy and small-scale processes.

A good summary of the understanding of the ACC as of 1972 is provided by the report "Southern ocean dynamics: A strategy for scientific exploration, 1973-1983" [Ad Hoc Working Group on Antarctic Oceanography, 1974]. The past decade has seen renewed emphasis on studies of the ACC, due largely to the International Southern Ocean Studies (ISOS) and the Polar Experiment (POLEX) South [Sarukhanyan and Smirnov, 1985; Sarukhanyan, 1985]. These programs encouraged and supported a wide variety of southern ocean studies. The ISOS program placed special emphasis on descriptions of fronts and energetics in the region of Drake Passage and southeast of New Zealand and on monitoring the transport of the ACC. The purpose of this review is to summarize the most important observational and theoretical findings of the past decade

regarding the ACC and, in some instances, to identify outstanding deficiencies in our knowledge and recommend studies to help fill these gaps.

We consider first, in section 2, the zonation of the southern ocean. Section 3 reviews attempts to estimate the transport of the ACC through Drake Passage and presents the best estimate to date. Much of the recent study of the southern ocean has focused on meridional exchanges, principally of heat but also of salt, momentum, and internal energy, by various processes. These studies are discussed in section 4. Observational studies of kinematics and selected dynamical quantities are considered in section 5. Section 6 outlines the dynamics of the circumpolar current as revealed by theoretical and numerical modeling studies. Finally, in section 7 we make some summary remarks and suggestions for future research.

2. ZONATION

Deacon [1937] noted that the isolines of salinity and temperature slope downward gradually in a series of steps toward the north across the ACC. Most of the ACC transport seems to be associated with two current cores separated by a transition zone in which the near-surface characteristics are intermediate between those of the Antarctic Zone south of the current and the Subantarctic Zone to its north. These current cores are fronts with pronounced horizontal gradients of density and other characteristics such as temperature T , salinity S , or nutrients; within the upper water column at least, characteristic relations (e.g., T - S) change abruptly across the fronts. Vertical sections of density across Drake Passage (e.g., Figure 3) show three fronts separating four water mass zones. From north to south these are called the Subantarctic Zone

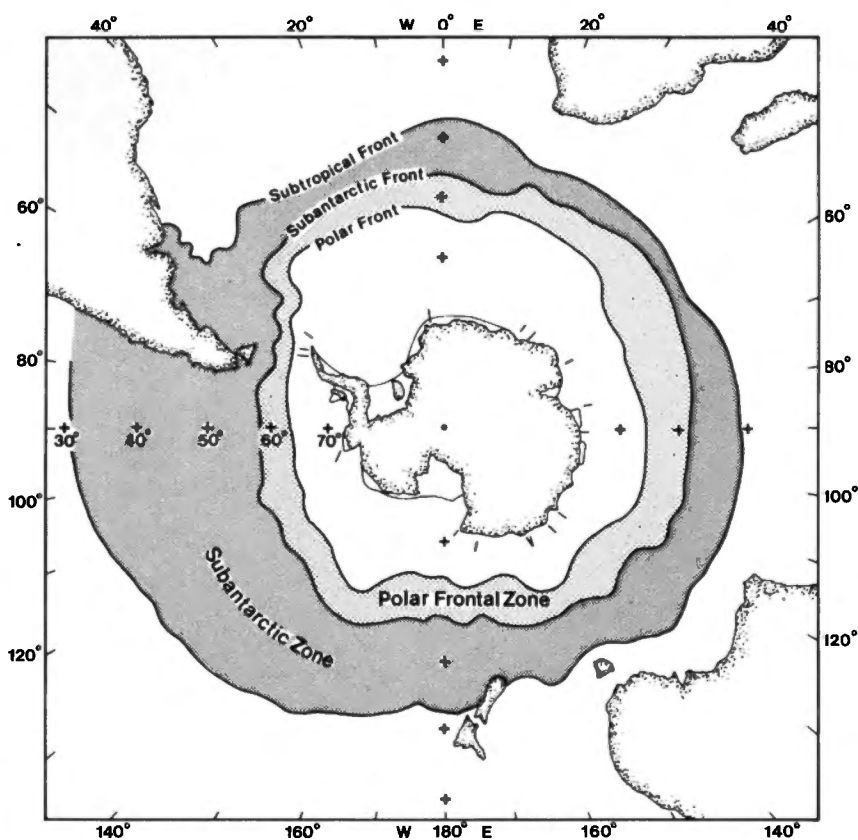


Fig. 4. Surface regimes of the southern ocean. Position of the Subtropical Front separating the subtropics from the Subantarctic Zone is after Deacon [1982]. Locations of the Subantarctic Front and Polar Front bounding the polar frontal zone are modified from a figure by Clifford [1983]. The Antarctic Zone is south of the Polar Front. Summer ice extent is shown near Antarctica, as are locations where a water mass transition near the continental slope has been observed [Clifford, 1983].

over horizontal scales of about 60 km and temporal scales of 20 days, to have characteristic amplitudes of 20 cm/s at 1000 m, to be vertically coherent over the observed depth range of 1000–5000 m, and to move southeastward at ~ 12 cm/s.

3. ZONAL TRANSPORT

Estimates of the volume transport of the ACC have frequently been used as inputs to, or observational checks on, circulation models. Realistic estimates of the transport and its variability can be of considerable value as a test of the ability of our models to account for pertinent dynamics: if a model cannot produce reasonable transport estimates, it must be deficient.

Early estimates of ACC transport that required the selection of a reference level varied greatly. Because the geostrophic shear in the ACC fronts extends practically to the bottom, middepth choices of zero-velocity reference levels resulted in westward deep flow under eastward flow and led to poor transport estimates. Also, when estimating transport at locations other than Drake Passage, it is difficult to separate the ACC flow from that due to adjacent currents. In the open ocean the southern limbs of the subtropical gyres and northern limbs of the subpolar gyres both flow eastward and are not easily distinguished from the ACC. Moreover, south of Australia and Africa other current systems, for example, the Agulhas Current, add to the confusion.

Geostrophic transport through Drake Passage relative to

3000 dbar for seven crossings made during 1975, 1976, 1977, 1979, and 1980 showed the baroclinic field to be relatively constant, with an average of 103×10^6 m³/s [Whitworth *et al.*, 1982]. This is consistent with estimates of relative geostrophic transports from earlier sections at Drake Passage [Reid and Nowlin, 1971]. Nowlin and Clifford [1982] showed that the transports associated with the three fronts in Drake Passage account for approximately 75% of the total baroclinic transport relative to 2500 dbar, though the fronts occupy only about 20% of the width of the passage.

The first estimates of ACC transport by using direct current measurements were made at Drake Passage in 1969 [Reid and Nowlin, 1971] and 1970 [Foster, 1972]. These were most confusing, but provocative, because the two independent estimates gave widely disparate results, 237×10^6 m³/s eastward and 15×10^6 m³/s westward.

A principal objective of the ISOS program was to obtain a yearlong record of ACC transport at Drake Passage. Initial effort went into the determination of vertical and horizontal length scales for velocity (for example, see Sciremammano *et al.* [1980]). As a result of that work, several preliminary transport estimates were produced from data collected in 1975: 110 – 138×10^6 m³/s [Nowlin *et al.*, 1977], $139 \pm 36 \times 10^6$ m³/s [Bryden and Pillsbury, 1977], and $127 \pm 14 \times 10^6$ m³/s [Fandry and Pillsbury, 1979]. All indicated eastward flow, and the agreement was good. Improved description of the ACC also showed that the disparate results of 1969 and 1970 were caused by undersampling of the reference velocities in the

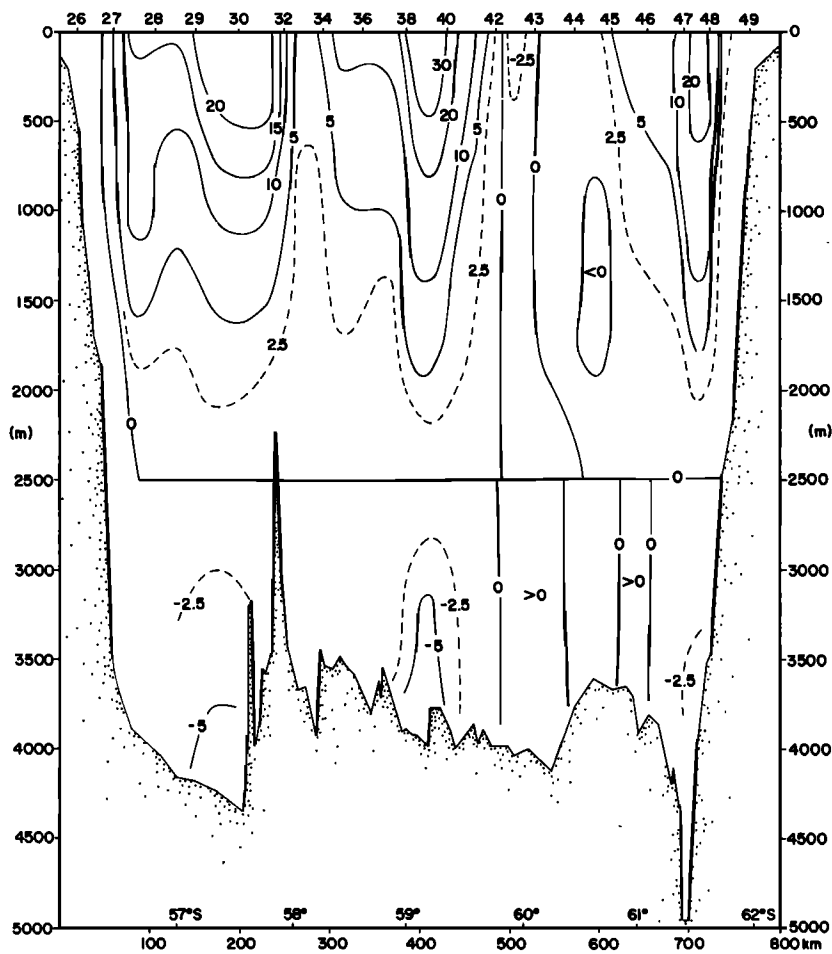


Fig. 5. Through-passage geostrophic speed (in centimeters per second) referenced to 2500 dbar for data collected at indicated station positions on R/V *Thompson* in February 1976.

presence of a highly structured current system consisting of meandering current cores.

The final ISOS transport product was a time series from January 1979 to January 1980, produced using data from pre-

cision pressure transducers and heavily instrumented moorings, simulating hydrographic stations, on both sides of the passage and from a large array of current meters moored on a line across the passage. Results have been described by *Whit-*

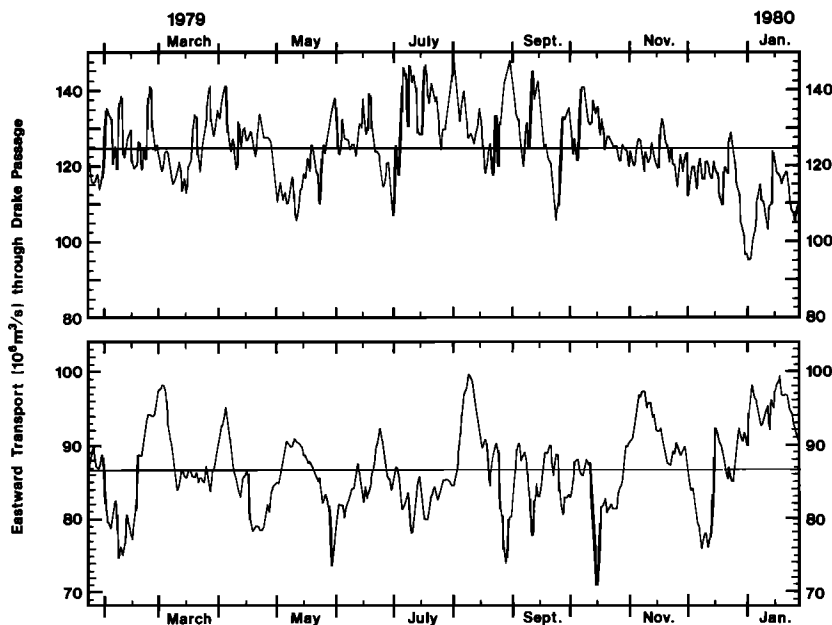


Fig. 6. Transport time series at Drake Passage in $10^6 \text{ m}^3/\text{s}$ [*Whitworth and Peterson, 1985*]: (top) net transport; (bottom) geostrophic transport in upper 2500 m relative to 2500 dbar.

worth [1983] and Whitworth and Peterson [1985]. The final net transport above 2500 m (Figure 6) has a mean of $125 \times 10^6 \text{ m}^3/\text{s}$ with a standard deviation of $10 \times 10^6 \text{ m}^3/\text{s}$. As can be seen by comparing the geostrophic transport above and relative to 2500 m (also shown) with the net transport, higher-frequency fluctuations occur in the barotropic mode, but 70% of the net is in the baroclinic mode.

Three shipboard density surveys of the passage were made in January 1979, April 1979, and January 1980 while the transport measuring array was in place. Fifteen to 18 stations were made along the current meter line. Referencing the geostrophic transport calculated from those data to the current observations at 13 moorings resulted [Whitworth *et al.*, 1982] in three net transport estimates: 117, 144, and $137 \times 10^6 \text{ m}^3/\text{s}$. Whitworth [1983] removed the transport below 2500 m from the first two of these estimates, obtaining 113 and $127 \times 10^6 \text{ m}^3/\text{s}$. These compared well with the net transport time series (from the monitoring array) averaged over the periods of the cruises: 112 and $121 \times 10^6 \text{ m}^3/\text{s}$.

Pressure records from 500-m depths on both sides of the passage were obtained also during the 2 years preceding the 1979 experiment. Wearn and Baker [1980] reported on the 1977 and 1978 results, which show a strong semiannual signal. These records have been added by Whitworth and Peterson [1985] to the 1979 records to extend the transport time series to 3 years. Comparison between net transport and transport estimated from pressure difference during 1979 shows a maximum difference of $24 \times 10^6 \text{ m}^3/\text{s}$ and suggests annual and semiannual fluctuations which are not phase locked. Additional pressure records from March 1981 to March 1982 show a pressure-derived transport ranging from 95 to $158 \times 10^6 \text{ m}^3/\text{s}$, with a standard deviation of $13 \times 10^6 \text{ m}^3/\text{s}$ [Whitworth and Peterson, 1985].

Although no monitoring of the ACC with direct measurements has been done at locations other than Drake Passage, estimates of ACC transport have been made elsewhere. Georgi and Toole [1982] estimated zonal heat and freshwater transports south of America, Africa, and New Zealand to obtain interocean exchanges for comparison with those of workers using different approaches. They calculated transport directly from hydrographic station data by taking the deepest sample depths as the reference level for each adjacent station pair, which resulted in transports of 140 and $125 \times 10^6 \text{ m}^3/\text{s}$ south of Africa and New Zealand, respectively. These geostrophic transports were adjusted using a spatially uniform reference speed so that the total volume transports matched the measured transport at Drake Passage (taken to be $127 \times 10^6 \text{ m}^3/\text{s}$). The differences in resulting eastward zonal transports through each opening gave a net gain of heat ($41 \times 10^{13} \text{ W}$) and loss of fresh water ($0.23 \times 10^6 \text{ m}^3/\text{s}$) for the Indian Ocean but losses of heat and gains of fresh water for the Atlantic Ocean ($23 \times 10^{13} \text{ W}$ and $0.14 \times 10^6 \text{ m}^3/\text{s}$) and Pacific Ocean ($18 \times 10^{13} \text{ W}$ and $0.08 \times 10^6 \text{ m}^3/\text{s}$). Calculations of the transports through Drake Passage of heat relative to 0°C ($13 \times 10^{14} \text{ W}$) and salt ($44 \times 10^{11} \text{ g/s}$), as well as of dissolved oxygen ($7 \times 10^{11} \text{ mL/s}$) and silicate ($104 \times 10^5 \text{ g/s}$), have recently been made using simultaneously measured property and absolute velocity fields from 1975 and 1979 (M. Giuffrida and W. Nowlin, personal communication, 1985). Such interocean exchanges of heat and fresh water, when combined with estimates of air-sea heat and moisture fluxes south of 40°S , gave Georgi and Toole the basis for estimating meridional heat and freshwater fluxes from the southern ocean into each of the three major oceans.

Fu and Chelton [1984] constructed time series of north-south sea level differences across the ACC from crossover sea level differences observed by Seasat during July to October 1978. The results reveal a general eastward acceleration of much of the ACC over that period with a decrease in the intensity of the cyclonic Weddell Gyre (Figure 7). This first direct observational evidence for large-scale coherence in the ACC demonstrates the great potential of satellite altimetry for synoptic observations of temporal variability.

There have been several attempts to relate the changes in net ACC transport, or across-passage pressure difference, at Drake Passage to wind stress over the southern ocean. Three years (1976–1978) of pressure difference across the passage were interpreted by Wearn and Baker [1980] in terms of fluctuations of the ACC. Then they related this transport time series to zonal wind stress integrated between 40° and 65°S over the southern ocean. A 28-day running mean filter was applied to the series. A strong correlation between the circumpolar wind stress and pressure difference was observed, in which the current lagged the integrated stress by about 9 days. This compared well with a simple model result of a 7-day lag which they also presented, suggesting that the pressure difference is forced globally rather than locally for periods longer than a month or that time changes in the ACC should be coherent around the circumpolar system.

Chelton [1982] then pointed out that the results were suspect on statistical grounds: for the procedures used, the coherence may have resulted because both series contain strong seasonal signals. Moreover, it can be seen from a later paper by Fu and Chelton [1984] that large-scale fluctuations in the ACC may not be coherent in circumpolar extent (see Figure 7 of this paper).

However, Whitworth [1983] compared the net transport at Drake Passage with the circumpolar-averaged zonal winds between 43° and 65°S for 1979, smoothing both with a 10-day low-pass filter. For periods between 16 and 24 days, the two series were coherent at the 95% significance level, and the phase implied that the wind leads the net transport by about 17 days. Whitworth noted that "neither (his nor Wearn and Baker's [1980]) time lag may be representative of the response time to forcing of the circumpolar current system as a whole" because localized disturbances which occur at different distances from Drake Passage during the year are included in the zonally averaged wind stress. Comparing the 3-year (1977–1979) pressure difference at 500 m with the circumpolar-averaged zonal wind stress, he has found (T. Whitworth, personal communication, 1985) that wind and pressure difference are coherent for periods between about 15 and 30 days, with wind leading by about 3 days. At this time one may conclude that different analysis procedures, longer time series, or different types of data will be required to resolve this issue.

4. MERIDIONAL EXCHANGES

Early in this century, warm deep water was shown to extend upward to shallow depths near Antarctica and was recognized as being related to the formation of an abyssal layer of cold antarctic water. Reid [1981] reviewed the development of this understanding. The surface modifications necessary to produce these dense waters require large heat exchange from the ocean to the atmosphere. An equivalent poleward heat flux must exist within the ocean.

We may examine this poleward heat flux by considering the

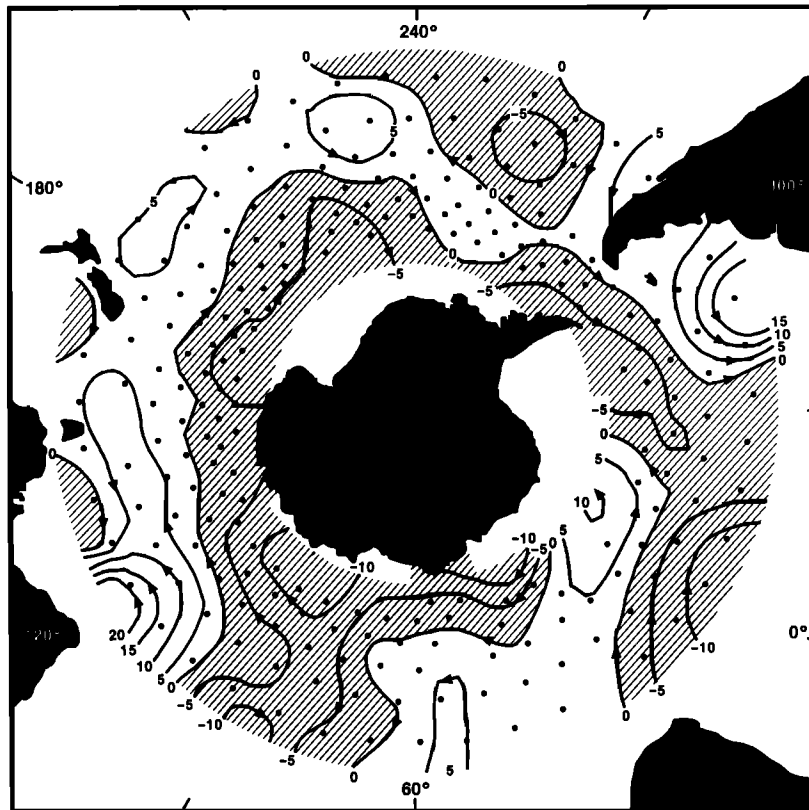


Fig. 7. The low-frequency (periods of longer than 20 days) change in sea level difference from Seasat crossover points during July to October 1978 [Fu and Chelton, 1984].

heat balance for the southern ocean south of the ACC in the following form:

$$Q = F_g + F_{Ek} + F_e + F_{bc}$$

where Q is the sum of the ocean-to-atmosphere heat exchanges south of the ACC and terms on the right hand side represent poleward heat fluxes across the ACC as follows: F_g , heat flux by mean geostrophic current, excluding deep boundary currents which are not well resolved; F_{Ek} , heat flux by surface Ekman transport; F_e , eddy heat flux; and F_{bc} , heat transport by deep boundary currents. Gordon and Taylor [1975] estimated the annual average heat loss from ocean to atmosphere south of the Polar Front to be 4×10^{14} W. A value of 54×10^{13} W for poleward ocean heat flux across 60° S was obtained by Gordon [1981]. This estimate is supported by Hastenrath [1982]. To obtain poleward heat flux across the Polar Front, Gordon subtracted the ocean heat gain between 53° (the average latitude of the Polar Front) and 60° S as given by the works of Zillman [1972] and A. F. Bunker (personal communication with Gordon, 1985). He obtained the value 3×10^{14} W, as was reported by deSzoek and Levine [1981]. This heat exchange is determined from climatological studies of surface conditions. Its value is important to the heat budget of the southern ocean (and that of the world ocean as well), but the uncertainty of our present estimate is likely large (perhaps 30 to 50%).

The advective geostrophic heat flux (F_g) across a circumpolar path was determined by deSzoek and Levine [1981], using a selection of historical hydrographic data taken to represent the mean conditions. The path chosen, which lies close to the mean path of the Polar Front, was that on which the vertically averaged potential temperature is 1.3° C. Integration

along such a path gives zero net barotropic flux across the path, to which deSzoek and Levine assign a worst case error of $\pm 1.0 \times 10^{14}$ W. For the baroclinic heat flux their circumpolar integration also gave zero, with a worst case error of $\pm 2.3 \times 10^{14}$ W.

Using average temperatures of the upper 100 m, taken from their hydrographic stations, and Ekman transport from a graphical display of annual mean zonal wind stress normalized by Coriolis parameter f [Taylor et al., 1978], deSzoek and Levine estimate a total equatorward heat flux due to Ekman transport (F_{Ek}) of 1.5×10^{14} W ($\pm 50\%$). The corresponding estimate of Ekman volume transport was 28×10^6 m³/s. The monthly mean winds compiled by Han and Lee [1981] were used by Clifford [1983] to compute average equatorward Ekman transport across circumpolar paths which she identified for the Polar, Subantarctic, and Subtropical fronts. Her value of 30×10^6 m³/s across the Polar Front is in good agreement with the estimate by deSzoek and Levine.

To summarize, ocean-atmosphere heat exchange south of the Polar Front and equatorward Ekman transport of warm surface water across the front together result in a mean heat loss of 4.5×10^{14} W from the ocean south of the ACC. The balancing poleward heat flux must be by oceanic processes. Because the effect of mean geostrophic flow (excepting perhaps deep narrow outflows) has been shown to be small by deSzoek and Levine, eddy processes and deep boundary currents remain as the prime candidates responsible for this poleward heat flux.

deSzoek and Levine [1981] point out that their calculations do not account for ageostrophic motions, such as deep boundary or interior currents with significant inertial or frictional terms. They also acknowledge that the coarse sampling

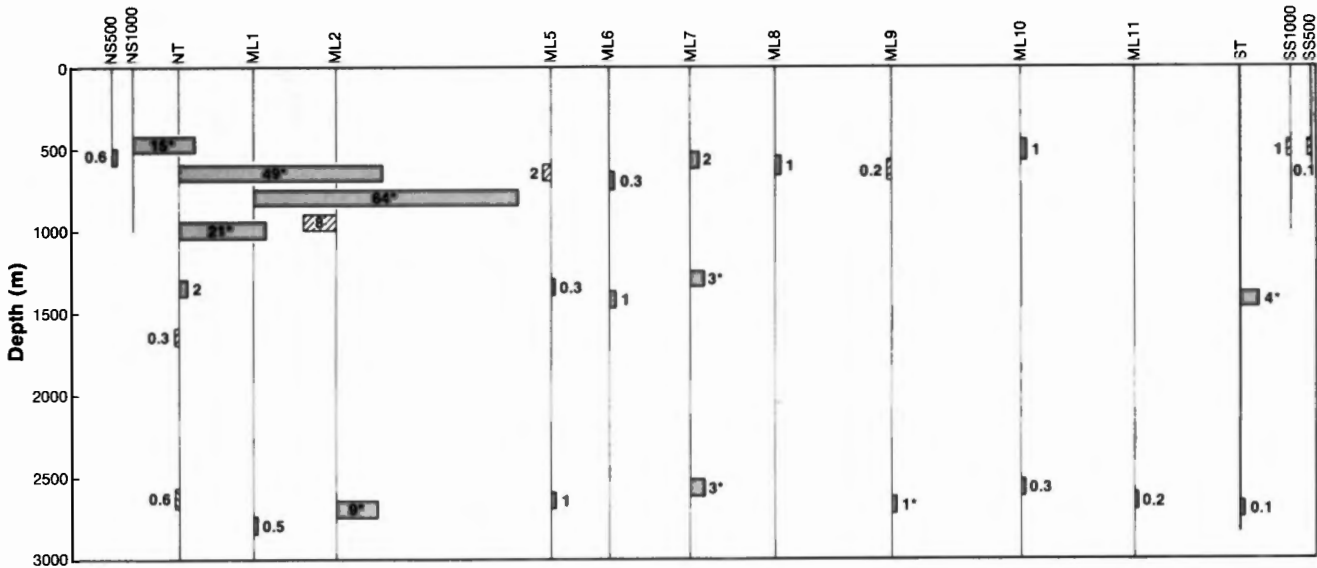


Fig. 8. Distribution of record length mean, across-stream eddy heat flux (in kilowatts per square meter) computed from 40-hour to 90-day band-passed temperature and velocity relative to the 90-day low-passed velocity. These yearlong 1979 moorings spanned Drake Passage from NS500 on the shelf south of Cape Horn to SS500 on the shelf off Livingston Island. Asterisks denote values significantly different from zero at a 95% confidence level. Equatorward fluxes are cross-hatched [Nowlin *et al.*, 1985.]

(46 blocks of stations to represent a 25×10^3 km long path) coupled with the rugged bottom topography along the path could have left some deep outflows unaccounted for. As an extreme example, they calculate a poleward heat flux of 1.5×10^{14} W for a deep outflow of 20×10^6 m³/s with an average potential temperature of -0.5°C . Direct monitoring of the major deep outflows is required to determine whether or not the heat transport by deep boundary currents is significant.

Bryden [1979] estimated meridional eddy heat flux from six nearly yearlong measurements of temperature and velocity from depths near 2700 m at locations spanning Drake Passage. Multiplying his average poleward heat flux estimate of 6.7 kW/m^2 by a depth of 4 km and a circumference (length of ACC) of 2×10^4 km gives a lateral flux of 5×10^{14} W. Sciremammano [1980] made additional estimates of eddy heat flux in Drake Passage. He compared estimates based on 1976 records from deep meters at northern, central, and southern passage locations with those obtained by Bryden using 1975 records from the same locations and found little difference in the northern and southern records. Using 1977 measurements from a cluster of five moorings in the central passage, Sciremammano extended Bryden's estimates over the depth range from 1000 to 2500 m. The variation in estimated eddy heat flux at this location over 3 years and all depths was large ($9\text{--}28 \text{ kW/m}^2$) with a mean of 17 kW/m^2 , which is considerably larger than Bryden's deepwater value of 6.7 kW/m^2 . It should be noted that these reported heat flux estimates are from records at least 5 months in duration that have not been corrected for temperature variations due to vertical motions of the instruments.

During 1979 a large yearlong array of current and temperature recorders was in place in Drake Passage. This data set was used by Nowlin *et al.* [1985] to examine the characteristics of eddy heat flux and its distribution at that location. The seemingly straightforward calculation of heat flux can produce misleading results unless measurement alias is removed and careful consideration is given to the frequency

bands and coordinate system selected for the analysis. When moorings blow over during periods of high current speeds, errors may be introduced into the eddy heat fluxes. Nowlin *et al.* [1985] corrected all the 1979 records from Drake Passage by using concomitant pressure time series and vertical temperature gradients (after the procedures of Rojas [1982]) and showed that failure to correct for instrument blow over could result in overestimates of meridional eddy heat flux by as much as 20%.

Although short time scale processes (such as tides, internal waves, and inertial oscillations) are routinely eliminated from heat flux estimates by low-pass filtering, low-frequency contamination of eddy heat fluxes is not usually considered. Long-period events can impose unwanted, dominating cross correlation (eddy heat flux) between fluctuation temperature and velocity. In Drake Passage, low-frequency variability in some current records is associated with sporadic lateral shifts of the fronts within the Antarctic Circumpolar Current. Defining an effective eddy time scale (40 hours to 90 days) and band-passing the current records before calculating eddy heat flux, Nowlin *et al.* [1985] obtained values which are more homogenous (consistent with one another) in direction and have higher statistical significance.

Finally, for the circumpolar current, they defined "poleward" eddy heat flux as that component perpendicular to the axis of the current, which forms a continuous but distorted band encircling Antarctica. Because the current direction varies in time, across-stream eddy heat flux was calculated relative to the 90-day low-pass direction. The resulting heat fluxes from 1979 are shown in Figure 8; only poleward fluxes were statistically significant. Values from the deep instruments and those in the southern and central passage are of the order of 1 kW/m^2 ; those in the northern passage are an order of magnitude larger. The average across-stream flux for all available instruments is 3.7 kW/m^2 poleward. This value, if representative of the average eddy heat flux through the ACC, yields a net (circumpolar) poleward heat flux due to eddy processes in the 2- to 90-day band of 3×10^{14} W.

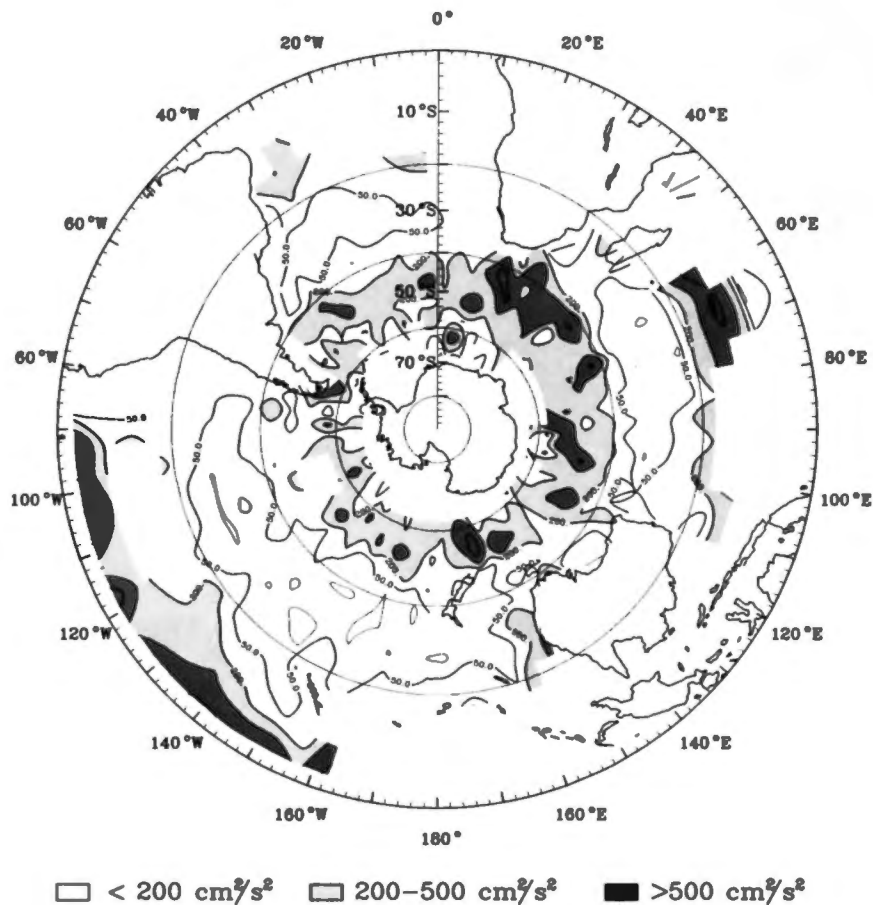


Fig. 9a. Kinetic energy of mean surface flow as indicated by FGGE buoy data [Patterson, 1985]. Hourly velocities are determined by spline fits to buoy positions. Velocities are averaged over $5^\circ \times 5^\circ$ squares.

Cospectra of fluctuation temperature and velocity show that heat flux is separated, on the average, into two frequency bands with corresponding periods between 100 and 40 days and between 16 and 10 days. This pattern compares favorably with the cospectrum from a 5-year bridged record from the central passage. Comparison with previous estimates in this region shows considerable differences, partly due to the use of different techniques. However, analysis of five 1-year records from a single location shows that interannual variability is large, which urges caution when interpreting the significance of isolated short-term estimates of eddy heat flux.

Bryden and Heath [1985] estimated meridional heat flux at the northern edge of the ACC using current and temperature records from a 2-year array moored southeast of New Zealand (near $49^\circ 30'S$ and $170^\circ W$). Their values varied from 1 to 35 kW/m^2 , falling within the range of values observed at Drake Passage. However, because of the long time scales of energetic variability, Bryden and Heath found the overall eddy heat flux was not statistically significant, although the portion in the 20- to 40-day band is significantly poleward.

The current rings which detach from the fronts of the ACC are assumed to account for much of the meridional transport across this current. Toward the end of section 5 are presented some estimates of heat, salt, and energy levels which have been estimated for individual rings.

Measurements have been made by T. Joyce and coworkers of small-scale structure at the Polar Front and within the Polar Frontal Zone both at Drake Passage [Joyce *et al.*, 1978] and southeast of New Zealand. The Drake Passage observations were used by Joyce [1977], in a model balancing

the lateral heat and salt diffusive exchanges across a water mass boundary with the vertical transport across boundaries of intrusions (interleaving), to obtain estimates of lateral diffusivity for vertical scales of interleaving between 1 and 100 m for an assumed range of vertical diffusivity. Assuming that the Drake Passage estimates are representative of the circumpolar front, they estimated that the intrusive heat flux across a 500-m-deep Polar Front would be 3.6×10^{13} W, or only about 10% of the required heat flux. On the basis of budget studies, the intrusive salt flux was estimated to be more significant in relation to the likely total salt flux across the ACC than was the intrusive heat flux in relation to the total heat flux. With the exception of the work by Joyce *et al.* on intrusive salt flux, few studies of other processes responsible for transport of salt across the ACC have appeared.

5. KINEMATIC AND DYNAMICAL ESTIMATES

Circumpolar Distributions

During the past 10 years the first estimates of circumpolar distributions of kinematic variability and surface kinetic energy have become available. Based on geopotential anomalies, ship drift records, surface drifter trajectories, and satellite altimetry, these distributions reveal regional differences in kinetic energy and variability over the path of the ACC inferred to be associated with current-topography interactions, interactions of the ACC with other current regimes, and boundary effects.

Wyrki *et al.* [1976] used observations of surface drift currents made by merchant vessels to calculate kinetic energy

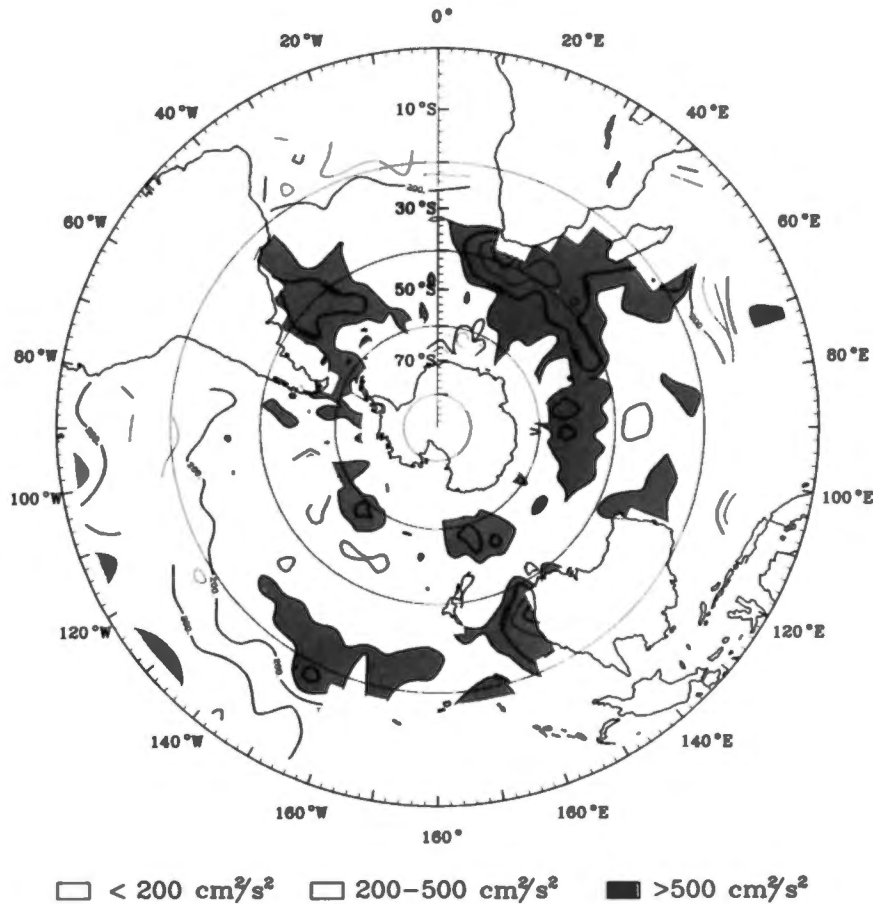


Fig. 9b. Eddy kinetic energy of surface flow from FGGE buoy data [Patterson, 1985] calculated by subtracting the mean kinetic energy from the total kinetic energy.

(KE) of the mean surface flow and of the fluctuations, interpreted as eddy kinetic energy (EKE), for the world ocean based on a 5° grid. Although the sparsity of data from high southern latitudes precluded good coverage of the ACC, a general distribution of KE of the mean flow and some indications of regions with unusually high EKE (e.g., Drake Passage and south of Africa) were revealed.

Using all available hydrographic stations, Lutjeharms and Baker [1980] carried out a statistical analysis of the mesoscale variability of the southern ocean. They presented patterns in the circulation intensity as expressed by the variance and horizontal structure function of the 0/1000-dbar dynamic height interval. The intensity of the mesoscale field was shown to be inversely proportional to distance from the mean ACC axis, suggesting that the Polar or Subantarctic fronts may be generating eddies over the length of the ACC. An upper limit of 150 to 250 km for the horizontal length scale of mesoscale turbulence was found for most of the southern ocean. Distinct patterns of high intensity of the variability were closely correlated with prominent topographic features on the sea floor.

Collinear altimeter data from the last 25 days of Seasat have been used in several studies of mesoscale variability including the region of the ACC. Colton and Chase [1983] selected three regions in which to study sea surface variability induced by interaction of the ACC with bottom topography: the Indian-Antarctic Ridge south of Australia, representing zonal flow along a zonal ridge; the Macquarie Ridge southwest of New Zealand, representing zonal flow over an isolated bump; and the Indian Mid-Ocean Ridge south of Africa, representing zonal flow over a meridional ridge. Residuals of col-

linear tracks from the mean profiles were calculated to represent variations of sea surface height. These transient features were studied to characterize length scales, dynamic height relief, and translational and surface geostrophic velocities. Cheney *et al.* [1983] presented a global distribution of mesoscale variability of the sea surface based on Seasat data. The high variability of the ACC extended nearly continuously around the southern ocean. Only in the extreme southeast Pacific and in the central South Atlantic were values of sea level rms variability less than 5 cm based on 2° gridded values. Values in excess of 6 cm were obtained over much of the ACC path, decreasing to the north and south. The largest variability again seemed to be associated with areas of major topographic relief.

Using data from approximately 300 drifting buoys deployed during the First GARP (Global Atmospheric Research Programme) Global Experiment (FGGE) during 1979, Garrett [1981] computed the mean and eddy kinetic energy on a 10° latitude by 10° longitude grid for the southern ocean. He used differences between buoy positions interpolated at 1200 UT each day to produce 24-hour averaged surface velocities. The results showed a general increase in KE levels, particularly that of the mean flow, associated with the ACC. However, the grid size was too large to permit much definition. Patterson [1985] fit spline functions to the FGGE buoy positions to obtain hourly time series of buoy velocities. For each $5^\circ \times 5^\circ$ grid, these were averaged, first to obtain monthly velocity components and then to obtain record length means used to construct the KE distribution of the mean flow presented in Figure 9a. The pattern shows the highly zonal distribution of

surface mean kinetic energy associated with the ACC. Relatively large mean KE values ($> 500 \text{ cm}^2/\text{s}^2$) appear within the ACC near major bathymetric features; relatively small values are found within the ACC in the extreme southeast Pacific and south of Australia, upstream of major topographic obstructions.

Most of the KE of the surface circulation is in the eddy field (Figure 9b). Eddy kinetic energy was calculated as the difference between total and mean kinetic energies for each $5^\circ \times 5^\circ$ box. Unlike the distribution of KE for the mean flow, which is zonal in nature, the highest values of EKE are associated with western boundaries, though secondary maxima do occur in patches within the zonal flow of the ACC shown in the mean KE pattern. The background meridional gradient seen in the high-frequency EKE is probably due to the influence of wind variance. The distributions seem generally consistent with the distributions of variability mentioned earlier, suggesting that the contribution to the variance by local wind effects is not large. However, this remains to be examined in detail.

Using trajectories of the FGGE surface drifters, Hofmann [1985] examined the circumpolar structure of the ACC. She found good correspondence between increased surface speeds and the historical locations of the Polar, Subantarctic, and Subtropical fronts. The mean near-surface speeds were approximately 40 cm/s for the PF and SAF, but only about 25 cm/s for the Subtropical Front. Greater drifter densities were found to be associated with the fronts than with the water mass regions which they separate, implying that there is horizontal convergence at the surface in these fronts. Regions with large bathymetric features gave the clearest indications of a banded current structure and the greatest meridional zonation in speed. This suggested to Hofmann that the lateral motions of fronts may be inhibited by bathymetry.

Site Specific Estimates

As a result of the ISOS monitoring efforts we now have estimates from the ACC of many kinematic properties, for example, integral time scales, temperature and velocity correlation lengths, and kinetic energy levels. These are, however, specific to two locations. A moored array was maintained from April 1978 to May 1980 near $49^\circ 30' \text{S}$, 170°W southeast of New Zealand. The site was chosen to be north of the ACC in the hope that northward eddy momentum flux, indicative of energy dissipation from the ACC, would be observed [Bryden and Heath, 1985]. In Drake Passage, five separate yearlong arrays of moorings were maintained during the years 1975–1980. Observations there spanned the ACC and are the basis for most of our present information. It should be pointed out that although by definition the entire ACC passes through Drake Passage, one cannot observe transitions in energy levels, scales, etc., equatorward of the current because the Subantarctic Front is typically located close to the northern boundary of the passage. However, the transition region poleward of the current can be observed in the southern half of the passage.

Within the ACC at Drake Passage, the typical time scale of dominant velocity fluctuations estimated as the first zero crossing of the autocorrelation function, varies from 1 to 4 weeks. For records below 2 km the average time scale is 2 weeks [Bryden and Pillsbury, 1977]. On the basis of data from a cluster of five moorings located near the southern edge of the Polar Frontal Zone in 1977, Sciremammano *et al.* [1980] found velocity fluctuations to be significantly correlated from

near surface to depths of somewhat more than 2000 m. There is typically bottom intensification over regions of locally rugged topography, as is demonstrated by the structure of vertical empirical orthogonal modes, leading to a decoupling between middepth and near-bottom currents in those locales. Sciremammano *et al.* found temperature fluctuations strongly correlated for all depth pairings observed except for instruments positioned near the northern extent of the temperature minimum layer (the Polar Front); there the temperature structure is characterized by inversions and isolated cold and warm features of small spatial extent.

Sciremammano *et al.* [1980] also examined the horizontal scales of velocity and temperature fluctuation by studying the plots of zero-lag, normalized cross correlation versus station separation. The spatial decorrelation scale was taken as the separation distance for which the correlation crosses zero. Velocity fluctuations in both through- and across-passage directions were narrow (30–40 km) normal to their flow direction and elongated (50–80 km) along the flow. Horizontal scales of temperature fluctuations were found to be approximately equal in through- and across-passage direction, with values of 80–100 km.

Inoue [1982] added to the 1977 data used by Sciremammano *et al.* the data from nine moorings in the 1979 array distributed across the passage. He examined vertical structure of 40-hour low-passed currents in terms of empirical and dynamic normal modes. The barotropic and first baroclinic modes dominated at all locations, together accounting for 83–99% of record variance. The first empirical mode, with more than 90% of the variance at most moorings, is surface intensified and appears to be a combination of barotropic and baroclinic modes. Time scales are 20–50 days for the first empirical mode and 7–20 days for the bottom-trapped second empirical mode. These relatively short time scales for variability at depth are consistent with the scales (average of 14 days) reported by Bryden and Pillsbury [1977] for depths from 2500 to 3100 m.

Inoue found the horizontal scales of coherence for the first two dynamic modes and the first empirical mode to be similar to scales described by Sciremammano *et al.* [1980]; scales are perhaps somewhat longer in the southern passage removed from the major flow of the ACC but are still shorter than 80 km, for which Bryden and Pillsbury [1977] found velocity fluctuations to be independent. Inoue found the scales of the second empirical mode to be smaller for longitudinal separations than estimated by Sciremammano *et al.*

By examining cross correlations for maximum lag, propagation speeds for the fluctuations can be estimated. Based on the midpassage arrays during 1976 and 1977, the propagation of fluctuations in temperature and velocity components is to the east in a through-passage direction (about 60°T). Propagation speeds average 12 cm/s (ranging from 9 to 20 cm/s), consistent with estimates of the propagation speeds of rings and meanders through the region.

Bryden and Heath [1985] have summarized the results of their study of mesoscale fluctuations using data from the measurement site southeast of New Zealand just north of the Subantarctic Front. They say that “energetic eddies are found to have typical amplitudes of 20 cm/s at 1000-m depth, to be vertically coherent throughout the water column, to vary over temporal scales of 30 d and horizontal scales of 60 km, and to propagate southeastward at about 12 cm/s.” They find their maximum value of eddy kinetic energy ($169 \text{ cm}^2/\text{s}^2$) at their

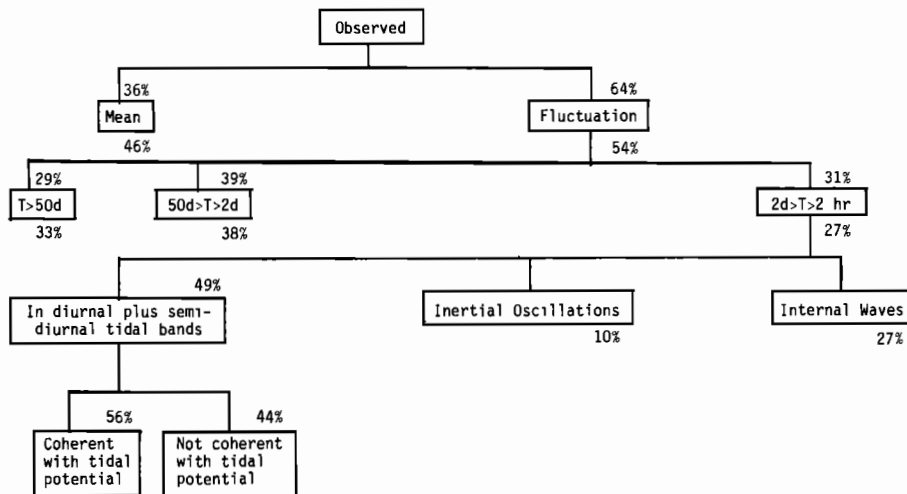


Fig. 10. Partitioning of kinetic energy of horizontal motions at Drake Passage. Fractions shown above boxes are averages for the entire passage; those below the boxes are averages from central passage locations [after Nowlin *et al.*, 1986].

shallowest record depth (1000 m). Though the horizontal scales from the Pacific location are somewhat larger than those in Drake Passage, the other results are in remarkable agreement, suggesting similar dynamical processes. Eddy kinetic energy values for fluctuations longer than 2 days in the northern Drake Passage, again just north of the Subantarctic Front, are over $140 \text{ cm}^2/\text{s}^2$ at depths below 2000 m and increase to over $200 \text{ cm}^2/\text{s}^2$ near 600–800 m.

The kinetic energy levels in the ACC at Drake Passage have been studied in considerable detail. Nowlin *et al.* [1981] examined 31 long records and found no significant interannual variability based on comparisons over 4 years, but they found large spatial variability. Examinations of the fifth year's records confirms this. The general trend is for mean KE values of $5\text{--}15 \text{ cm}^2/\text{s}^2$ at 2500–3000 m increasing upward to values near $300 \text{ cm}^2/\text{s}^2$ at 500 m. Eddy kinetic energy values for fluctuation periods of longer than 3 days are rather uniform in the southern and central passage (near $20 \text{ cm}^2/\text{s}^2$), increasing northward through the ACC to maximum values at the northernmost moorings. (Total EKE in the deep water increases across the passage by a factor of 5.) The average partitioning between mean and eddy kinetic energy and between three frequency bands for EKE is shown in Figure 10. Studies of the principal short-period tides [Nowlin *et al.*, 1982] and of internal and near-inertial oscillations [Nowlin *et al.*, 1986] have led to estimates of the fractions of eddy kinetic energy for periods of 2 hours to 2 days which are associated with these phenomena at Drake Passage (Figure 10).

Numerous current rings and meanders have been reported at Drake Passage. On several occasions, rings have been observed during formation (to date, always in the Polar Frontal Zone). Shipboard observation of cold core rings in the process of formation from the Polar Front has occurred twice, as was reported by Joyce and Patterson [1977] and Peterson *et al.* [1982]. When last observed, the ring tracked by Peterson *et al.* appeared to be pushing northward through the Subantarctic Front. On the basis of weekly synoptic maps depicting changes in frontal positions for 1979 (constructed using temperature and velocity data from 15 moorings in the northern and central Drake Passage), Hofmann and Whitworth [1985] described the formation and movement through the passage of three cold core rings from the Polar Front and one warm core

ring from the Subantarctic Front (as well as several large meanders). All of these rings had radii of the order of 50 km, surface speeds consistent with their formation from the ACC fronts, and deep-reaching density structure, and they moved northward or northeastward at speeds of 5–10 cm/s. All but one appeared to be steered by bottom topography.

Many individual ring sightings have been reported, not all in Drake Passage. For example, Gordon *et al.* [1977b] interpreted 1975 hydrographic observations in the eastern Scotia Sea as indicative of a ring of subantarctic water within the Polar Frontal Zone, and Savchenko *et al.* [1978] observed a larger (140-km diameter) cyclonic ring in the Polar Frontal Zone south of Australia in 1977.

Pillsbury and Bottero [1984] interpreted the records from a midpassage location south of the Polar Front in the Antarctic Zone as showing that five cyclonic rings and one anticyclonic ring passed the location between June 1975 and January 1976. The cyclonic rings had the properties of the continental water near the Antarctic Peninsula and were likely derived from the Continental Water Boundary; the anticyclonic (warm core) ring is believed to have separated from the Polar Front. The rings had diameters of from 30 to 130 km, extended vertically to at least 2500 m, and had maximum spin velocities of about 20 cm/s at 1000 m and 10 cm/s at 2500 m.

A ring census has not proved feasible using satellite images of temperature or color obtained from visible measurements because of the very high incidence of cloud cover. Based on the studies of time series during 1975 and 1979 at Drake Passage, however, the number of ACC rings in existence at any time must be large if these years are typical and the Drake Passage is characteristic of the circumpolar situation.

Available heat and salt anomalies, available potential energy, and kinetic energy of various rings have been estimated and reported [Joyce *et al.*, 1981; Peterson *et al.*, 1982; Pillsbury and Bottero, 1984]. Heat and salt anomalies were calculated by comparing the temperature and salinity within density intervals in the rings with characteristics at the same densities within the waters surrounding the rings. Available potential energies were calculated following the suggestions of Reid *et al.* [1981]. Vertical sections of available heat and salt anomalies are shown by Joyce *et al.* [1981] and Peterson *et al.* [1982], and the former picture kinetic and available potential

TABLE 1. Estimates of Property Anomalies for Some Southern Ocean Current Rings

| | Joyce <i>et al.</i> [1981]* | Peterson <i>et al.</i> [1982]† | | Pillsbury and Bottero [1985]‡ | |
|-------------------------------|--------------------------------|------------------------------------|------------------------------------|----------------------------------|-----------------------|
| | | Relative to PFZ Characteristics | Relative to SAZ Characteristics | Anticyclonic | Cyclonic |
| Available potential energy, J | 5.1×10^{14} | ... | ... | 0.9×10^{14} | 3.9×10^{14} |
| Kinetic energy, J | 3.4×10^{14} | ... | ... | 0.5×10^{14} | 1.5×10^{14} |
| Heat anomaly, J | 1.2×10^{19} | 0.8×10^{19} | 3×10^{19} | 1.0×10^{18} | -1.9×10^{18} |
| Salt anomaly, kg | 2.5×10^{11} | 2.0×10^{11} | 8×10^{11} | ... | ... |

*Anomalies, relative to Polar Front Zone characteristics, were integrated between $\sigma_t = 27.0$ and 27.7 (approximately sea surface to 1500 m in PFZ) based on a section through a 1975 cyclonic ring in the Polar Frontal Zone. Kinetic energy is based on geostrophic speeds relative to 2800 dbar.

†Anomalies integrated from $\sigma_t = 27.0$ to 27.8 (approximately sea surface to 2500 m in the PFZ) based on a vertical section through a 1979 cyclonic ring in the Polar Frontal Zone.

‡Values of velocities and temperatures obtained from a symmetric ring model with parameters determined by time series observations of these parameters. Values shown on the left are for an anticyclonic ring of Polar Frontal Zone water and those on the right are the average for five cyclonic rings of continental water, all observed in the Antarctic Zone. Anomalies relative to Antarctic Zone characteristics were integrated down to 3500 m as a nominal bottom depth.

energies and potential vorticity are shown as well. In Table 1 we present for comparison integrals over the ring volumes given in these three papers. Note that rings from two different fronts (Polar Front and Continental Water Boundary) are given and that anomalies are estimated relative to the characteristics of different water mass zones. Each set of authors speculates on the consequences of ring formation for meridional transfers across the ACC.

Several researchers have analyzed the stability of flow in Drake Passage; most found the flow, even though defined by different measures, to be baroclinically unstable. Furthermore, the characteristics of the instability are similar for the various analyses. Fandry [1979] used the average of all current observations from Drake Passage for the years 1975–1977 to obtain a mean speed and mean shear as a function of depth. The Brunt-Väisälä frequency was estimated from hydrographic data. Fandry found the unstable waves to have lengths of between 123 and 390 km and the most unstable wave to have a growth rate of 25 days. Bryden [1979] analyzed the stability of flow in central Drake Passage using repeated hydrography and a single current meter mooring to estimate the Brunt-Väisälä profile and the mean current shear, respectively. The flow was found to be unstable, and a detailed comparison of theoretical expectations with observations yielded mixed results. However, energy conversion was estimated from the data and found to be within a factor of 2 of the estimated wind energy flux from the atmosphere. Peterson *et al.* [1982] examined the necessary condition for baroclinic instability based on the vertical shear of zonal geostrophic current and the hydrostatic stability calculated for each of the four water mass zones in Drake Passage by using 1976 hydrographic data. They found the necessary conditions for instability met in each of these zones even though they are between the current cores (or fronts) and have relatively weak vertical shear. Using the same data set, they also found necessary conditions for barotropic instability adjacent to each of the three fronts in Drake Passage.

Wright [1981] analyzed observations from a compact cluster of current meters in central Drake Passage (part of the First Dynamic Response and Kinematics Experiment (FDRAKE 77) observations). Current shear and Brunt-Väisälä profiles were obtained from the 1977 current observations and

hydrography. The stability problem was solved in terms of east-west propagations with sinusoidal structure in the north-south direction. The ninth north-south mode, with a width scale of 78 km, was analyzed for stability. The most unstable wave had a growth rate of 16 days and a length scale of 143 km. Energy conversion estimates from the observations agreed well with characteristics of the most unstable wave from the model.

Inoue [1985] used the extensive Dynamic Response and Kinematics Experiment of 1979 (DRAKE 79) observations to consider the question of flow stability. He carefully considered the characteristics of the different water mass zones in Drake Passage and found that all of the zones are baroclinically unstable. The fastest-growing wave has a length decreasing from 177 km in the northern passage to 91 km in the southern passage. Growth rates are slow (15–40 days) between the fronts and fast (3–5 days) in the fronts. The instability is a mixture of barotropic and first baroclinic modes, with two thirds of the energy going to the barotropic mode.

In a study of current rings in Drake Passage, Pillsbury and Bottero [1984] examined three long current records (at 1020, 1520, and 2520 m) from a single mooring in the Antarctic Zone. This is the same mooring from which Bryden's [1979] analysis of the complete 12-month data set indicated conditions favorable for the production of mesoscale waves by means of baroclinic instability. Deleting those portions of the records containing rings, Pillsbury and Bottero found that for the period from February to October 1975 the conditions were indicative of energy transfer from eddy kinetic energy to available potential energy. Transfer rates (calculated following Wright [1981]) were of the order of 2×10^{-5} ergs/cm³/s, with the values decreasing with increasing depth. They concluded it was unlikely that the six observed rings originated under the conditions observed at that site in the Antarctic Zone because the conditions did not support the formation and growth of eddies through baroclinic instability.

Several observational studies have considered, peripherally, to what extent the ACC is in geostrophic balance. Using 1975 measurements at Drake Passage, Nowlin *et al.* [1977] demonstrated that geostrophic shear from pairs of hydrographic stations agrees with measured shear at positions between the stations if the direct current measurements are appropriately

averaged. The same procedure was used successfully by *Whitworth et al.* [1982] in combining 1979 station data and direct current measurements to estimate ACC transport.

Using data from the 1979 ISOS transport experiment, *Whitworth and Peterson* [1985] formed a time series of the difference between through-passage velocity components at 500 m averaged across the passage and those at 2500 m. They compared this series with the time series of 500- to 2500-m geostrophic shear obtained from heavily instrumented vertical moorings at the northern and southern edges of the passage. (The time series were smoothed with a 10-day low-pass filter; the series lengths were approximately 12 months.) Even though the estimate of directly measured shear may not be a good representation because some current meters were lost, leaving gaps, the two shear estimates are coherent (at the 95% level) and in phase for periods between about 25 and 50 days, suggesting that fluctuations in the ACC are approximately in geostrophic balance.

6. THEORY AND MODELS

Basic Dynamical Problem of the ACC

Hidaka and Tsuchiya [1953] applied the basic ideas of the developing theory of wind-driven ocean circulation to the southern ocean. A constant wind stress was applied as the driving force; lateral and vertical viscous effects provided the dissipation. With reasonable choices for the friction coefficients, the transport of the resulting circulation was about 1 order of magnitude too large. The reduction of the transport to reasonable levels required viscous coefficients approximately 100 times the largest "acceptable" values. The basic dynamical balance in the ACC appeared to be fundamentally different from the balance in a closed basin.

McWilliams and Chow [1981] developed an eddy-resolving, three-layer model of a wind-driven zonal channel, which is equivalent to the *Hidaka and Tsuchiya* calculation but with no explicit turbulence closure hypothesis. Eddies due to baroclinic instabilities appeared in the flow, and those eddies redistributed momentum. It is possible to calculate effective eddy viscosities from correlations of the velocity fluctuations. The eddy viscosities calculated from the model were nearly equal to the values used by *Hidaka and Tsuchiya* to get reasonable transports. Therefore it appears that subgrid-scale viscous dissipation, in the absence of lateral and bottom topography, cannot be the only process balancing the forcing of the surface wind stress.

The basic problem is to find a dynamical balance for the ACC that allows for observed surface wind stress as a driving force while maintaining reasonable transport values. Transport is a key variable used to test the applicability of models to the prototype. Indeed, this observation has such importance that considerable effort was expended in the late 1970s to determine the transport of the ACC at Drake Passage. We now have a 1-year observed time series of this transport and 3 years of additional good estimates modeled from across-passage pressure differences [*Whitworth and Peterson*, 1985]. Given this improved estimate of the transport, it is appropriate now to reconsider the theories advanced for the dynamical balance within the ACC.

Four dissipative mechanisms have been considered as possible balances for the wind stress. Simply stated, these are form drag due to bottom topography [*Munk and Palmén*, 1951],

baroclinicity [*Fofonoff*, 1955], effect of continental land masses [*Stommel*, 1957], and discharge of water from Antarctica [*Barcilon*, 1966, 1967].

Even before the *Hidaka and Tsuchiya* [1953] paper, a dynamical model of the ACC was advanced by *Munk and Palmén* [1951], who realized that viscous dissipation was insufficient to balance the wind stress. They suggested that form drag, due to flow over bottom topography, provides the force necessary to balance the wind. Moreover, they estimated that the drag force due to the four largest ocean ridges can balance the observed surface stress.

The study by *Fofonoff* [1955] is a direct extension of the work of *Hidaka and Tsuchiya* [1953] to include stratification and forcing by surface buoyancy flux which drives flow westward against the prevailing flow in the ACC. The geometry is a zonal channel, and both vertical and horizontal viscous effects are included. The transport calculated for various combinations of surface forcing shows that stratification actually increases the transport because it causes the wind-driven flow to be reduced near the bottom, thus reducing the effectiveness of bottom viscous dissipation. The major conclusion is that the addition of baroclinicity is not sufficient to form a proper balance for a zonal model of the ACC.

Stommel [1957] was first to observe that the ACC does not flow in a zonal channel at all but that only a narrow band of latitudes is not blocked by land barriers and that even this band is blocked by bottom topography that comes within 1000 m of the surface. He maintained that most of the flow is Sverdruplike, since pressure differences are allowed across continental boundaries. He further argued that viscous dissipation takes place in the western boundary currents that exist along land boundaries, with the principal dissipation occurring downstream of Drake Passage along South America.

The discharge of water from the Antarctic continent can drive a westward flow, thereby reducing the transport of the ACC [*Barcilon*, 1966, 1967]. As water is discharged from the continent, a free surface slope develops (down to the north) which drives a westward current. There is a strong amplification effect, so the circulation created is 100 to 1000 times the discharge. Even this amplification is not sufficient to reduce the unrealistically large eastward transport calculated by *Hidaka and Tsuchiya* [1953] to result from the wind driving. Furthermore, the discharge must come from melting snow and ice, so the ACC should show strong seasonal transport variations. The observed variations are not strong enough, and though this mechanism may be important near the continent, it seems to be of little consequence in ACC dynamics.

Simplified Dynamical Models of the ACC

Dynamical models of the ACC discussed in this paper are partitioned into three categories: simplified models, world ocean models, and mesoscale models. The simplified models address either reduced dynamics or a limited region of the ACC. World ocean models necessarily contain the ACC, but only large-scale (hundreds of kilometers) processes can be included because of computer limitations. Mesoscale models address effects of dynamic instabilities and bottom topography on flow in zonal channels. Each type of model considers some part of the dynamics of the ACC, and these results will lead to more realistic dynamical understanding of the ACC.

Wyrtki [1960] made a detailed Sverdrup transport calculation for the southern ocean using his best estimate for the

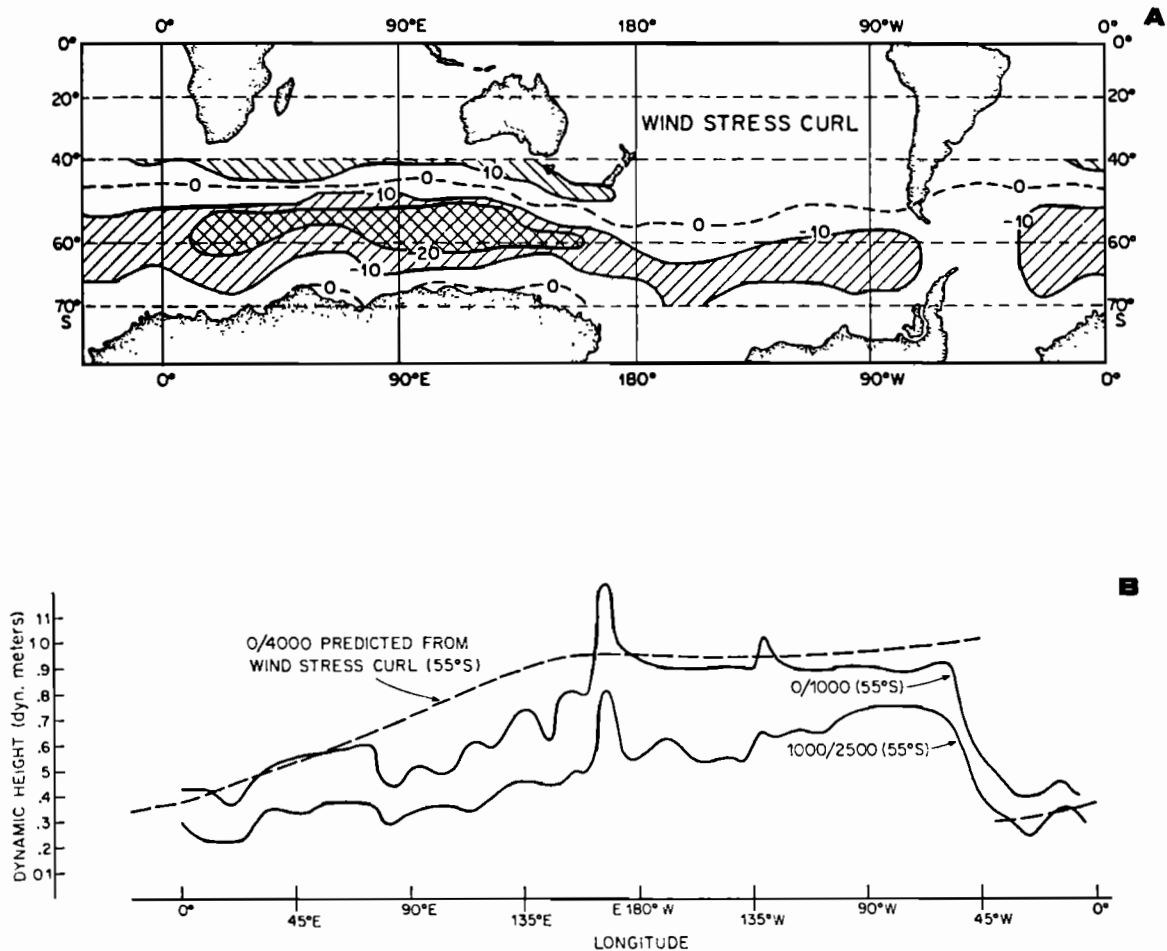


Fig. 11. (a) Wind stress curl calculated by Taylor [1978] from the data of Jenne *et al.* [1971]. Contours are 10^{-9} dyn/cm^3 . (b) Dynamic height at 55°S as a function of longitude from the data of Gordon *et al.* [1978] and predicted dynamic height from wind stress curl data shown in Figure 11a [from Baker, 1982].

meridional structure of the zonal wind stress based on the meager data available at the time. The transport was integrated from the western coast of South America (the eastern boundary). A linear transport distribution was chosen for Drake Passage matching the presumed structure of the flow. The resulting flow pattern coincided with the large-scale properties of the flow as it was then understood. In general, the model ACC shifted to the south as it flowed eastward through the Indian and Pacific oceans. Despite its correspondence with observations, this model is unsatisfying because the ACC transport is imposed on the solution and the important question of the "non-Sverdrup" dynamics that take place near Drake Passage is not addressed.

Using the wind climatology of Jenne *et al.* [1971] and Han and Lee [1981] and the hydrographic station data selected by Gordon *et al.* [1978], Baker [1982] made a similar Sverdrup calculation of the wind-driven flow across 55°S (chosen because it is at approximately the tip of South America). If the Sverdrup balance is appropriate in the southern ocean, then the water driven south across this latitude from 40°W eastward to 70°W should approximately balance the ACC transport through Drake Passage, which then turns northward before flowing to the east again near 40°W . In Figure 11 are shown circumpolar distributions of wind stress curl and of dynamic height estimates at 55°S as functions of longitude. Integrating the 0/3000-dbar dynamic topography along 55°S

yields a southward transport between 40° and 90°W of $113 \pm 20 \times 10^6 \text{ m}^3/\text{s}$, which Baker contrasted with $103 \pm 13 \times 10^6 \text{ m}^3/\text{s}$ geostrophic transport through Drake Passage above and relative to 3000 m estimated by Whitworth *et al.* [1982] from seven ISOS density sections. Using the Sverdrup balance, Baker integrated the wind stress curl again along 55°S to obtain a southward transport of $190 \pm 60 \times 10^6 \text{ m}^3/\text{s}$. Though somewhat large, this value may be compared with the four direct measurements of total transport through Drake Passage by Whitworth *et al.* [1982] of 117, 144, and $137 \pm 6-15 \times 10^6 \text{ m}^3/\text{s}$ and by Nowlin *et al.* [1977] of $124 \pm 15 \times 10^6 \text{ m}^3/\text{s}$. This calculation indicates that the southern ocean is forced by wind stress curl which pushes water across latitude lines.

The wind-driven transport of the ACC is presented by Kamenskovich [1962] as a combination of barotropic and Ekman-driven flows. Geostrophic stream lines are used to evaluate flow through Drake Passage. No stratification is included, but smoothed bottom topography is allowed. Vertical friction is used to balance the wind stress. The flow obtained agrees with dynamic topography, and the transport is reasonable ($130 \times 10^6 \text{ m}^3/\text{s}$). The calculation shows the importance of bottom topography in determining circulation in the southern ocean.

Rattray [1964] analyzed the time dependent behavior of a two-layer fluid on a beta plane. The linear, primitive equations are converted to modal (internal and external) form and ana-

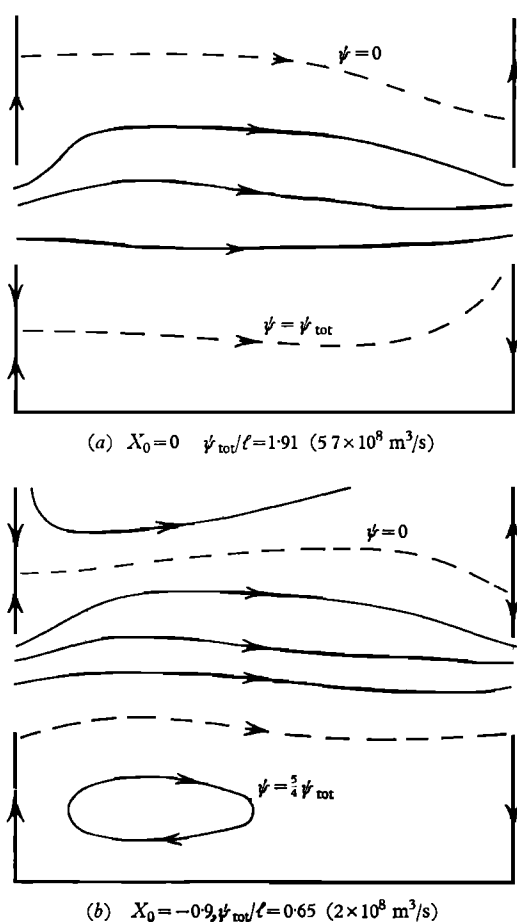


Fig. 12. Numerical solution for a model of the ACC with meridional walls representing South America and the Antarctic Peninsula [from Gill, 1968]. The windstress is zonal and is the sum of a constant (X_0) and a part that varies sinusoidally with y . For the case in Figure 12a, $X_0 = 0$ and the transport is $570 \times 10^6 \text{ m}^3/\text{s}$. For the case in Figure 12b, a westward stress ($X_0 = -0.9$) is applied, resulting in a reduced transport ($200 \times 10^6 \text{ m}^3/\text{s}$) and an enhanced polar gyre. (Taken from Figure 5 of Gill [1968].)

lyzed for oscillatory solutions. A dispersion relation, representing two gravity waves and one Rossby wave, is obtained for waves having sinusoidal structure in both horizontal directions. For parameter values representative of the southern ocean, the Rossby wave periods range from a few weeks to several months for the external mode and from years to thousands of years for the internal mode.

Devine [1972] included stratification in an inviscid, wind-driven model of the ACC. A "porous plug" supporting a pressure difference is placed in Drake Passage to avoid explicit consideration of the western boundary currents. The calculation is a combination of a Sverdrup model and a thermocline model because the advection of temperature is included. The resulting governing equation is solved by assuming that the linear and nonlinear parts vanish separately, which implies that only the baroclinic flow advects temperature variations, that the horizontal flow is nondivergent, and that vertical advection of temperature is balanced by vertical diffusion. The resulting ACC transport of $260 \times 10^6 \text{ m}^3/\text{s}$ is split about evenly between barotropic and baroclinic parts. The coldest surface temperatures occur east of Drake Passage, across which there is a strong east-west temperature gradient (about 2°C). This model does not address the mechanism that balances the wind stress.

The first complete model of the ACC [Gill, 1968] filled in the details of the dynamical hypothesis advanced by Stommel [1957]. The model had linear dynamics, a flat bottom, homogeneous fluid, and linear bottom friction; it is Stommel's basin model with a recirculating gap. The model equations are solved numerically and through a perturbation (boundary layer) technique. The wind is assumed to be zonal with a structure composed of the sum of a constant stress (X_0) and a part with sinusoidal north-south structure. Examples of the solution for two values of X_0 (Figure 12) show that the model generally agrees with observations. A western boundary layer develops, and most of the ACC enters this layer after flowing through the gap. Furthermore, the currents in the northern side of the gap are stronger than those in the south, as is observed in Drake Passage. While the resulting transport values are larger than measured transports, they are much smaller than transports in strictly zonal models with the same values for the viscosities. This result shows the importance of meridional boundaries on the flow in the southern ocean.

Schulman [1970] presented a numerical version of the Gill [1968] model including the effects of bottom topography and nonlinearity. A stretched grid, primitive equation model is used, with the finest resolution (50 km) occurring in Drake Passage and along the straight continental boundary and with increasingly coarse resolution in the rest of the southern ocean. For a flat bottom (5 km deep), the transport ranges from 70 to $200 \times 10^6 \text{ m}^3/\text{s}$ for various values of the bottom friction coefficient. The addition of nonlinear terms to the model dynamics changes the appearance of the flow; in particular, the ACC overshoots the east coast of South America before turning north. However, the total transport of the ACC is not greatly changed by nonlinear effects. The most important result of this calculation is the effect of topography in Drake Passage on the total transport. The topography is added in four pieces: continental slopes (1 km deep), Scotia Ridge and the South Sandwich Islands (3 km deep), a shallow plateau in Drake Passage (2 km deep), and the continental shelf east of South America (1 km deep). When each of these features is separately added to the model, it is found that the plateau topography in Drake Passage has the strongest effect on the transport, reducing it from 130 to $25 \times 10^6 \text{ m}^3/\text{s}$, while the other topographies cause only a 10 to 20% reduction. With all four pieces included, the total transport is $20 \times 10^6 \text{ m}^3/\text{s}$. The implication of this first complete model with topography is that bottom topography is certainly effective, at least in a one-layer case, in reducing the total transport.

The analytical study of Johnson and Hill [1975] also shows the bottom topography to play a major role in reducing the wind-driven transport. A three-dimensional, homogeneous model with vertical friction is integrated along geostrophic contours passing through a recirculation gap in a rectangular basin model. For topographic relief that is 20% of the total depth, transport may be reduced by as much as 85% (relative to the flat bottom case). Johnson and Hill argue that the reduction in transport comes from increased bottom dissipation due to faster currents produced as water moves through shallower regions, such as Drake Passage.

The interaction of stratification and topography was considered by Gill and Bryan [1971] by using an eight-level model of flow in a flat-bottomed, rectangular basin driven by zonal winds and an imposed surface temperature distribution. Two forms were considered for the gap through which recirculation passes: extending to basin depth (deep gap) and extending to

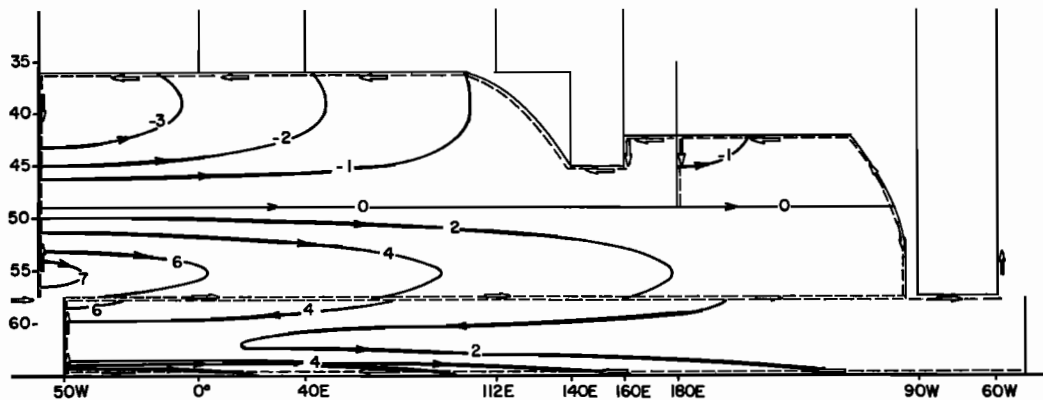


Fig. 13. Transport streamfunction for the southern ocean as determined by Veronis [1973] from a Sverdrup calculation for a two-layer world ocean model forced by the mean wind stress distribution of Hellerman [1967]. This calculation allowed the interface to reach the sea surface, exposing the lower layer directly to wind stress. The dashed curve along the northern edge of the region pictured is the trace of that interface on the sea surface; thus the entire southern ocean is modeled as one (lower) layer driven directly by the wind.

only half the basin depth (shallow gap). For the second case the partial wall mimics the shallow area in Drake Passage. The Coriolis parameter is chosen to be one tenth of the correct value so that the numerical solution will be stable with a coarse horizontal resolution but without the need for excessive friction. The vertically integrated flow compares well with the analytical model of Gill [1968]. The transport in the model ACC for the deep gap case is $300 \times 10^6 \text{ m}^3/\text{s}$, while for the shallow gap case it is $836 \times 10^6 \text{ m}^3/\text{s}$. The increase in transport with topography is shown to be due to a pressure difference across the wall in Drake Passage which comes from a temperature difference (warm water to the west and cold water to the east). It is not clear whether this effect is important for topographic barriers with finite widths.

Clarke [1982] analyzed the dynamics of wind-driven flow in a zonal channel with a flat bottom. The emphasis of the study is on the interaction of large-scale wind forcing on the large-scale currents. Scale arguments are based on east-west scales of 7000 km and north-south scales of 700 km. The full dynamics are reduced to the equations governing thermocline dynamics, and a similarity solution is proposed which partitions the flow into baroclinic and barotropic parts. The results of the study indicate that barotropic flow should respond mainly to the zonally averaged (zero zonal wave number) wind with a time lag of 10 or so days. This spindown time is too rapid to be due to bottom Ekman layers, so it is assumed to be due to Rossby wave drag on small scale variations in bottom topography. The barotropic part of the transport, according to Clarke, should vary by about 65% over a year (measurements show a maximum variation to be about 40% of the mean [Whitworth *et al.*, 1982]).

Much recent analysis of large-scale circulation is from the point of view of inviscid flow that conserves potential vorticity. In closed basins the wind forcing must deflect the flow sufficiently to cause lines of constant potential vorticity to close upon themselves; otherwise, no circulation is possible. In the southern ocean there is the possibility of some potential vorticity lines circling the globe (the ACC) allowing zonal flow that need not be strongly forced. Haynes [1985] considers how a gyre and a free zonal current interact. His analysis considers two-, three-, and four-layer models in addition to a calculation for continuous stratification. The occurrence of the free zonal flow allows penetration to the bottom of the effect of wind forcing. In the absence of the zonal flow, the penetra-

tion depth of the wind forcing is determined by the strength of the wind. The interaction of the zonal current and the wind driven gyre give rise to (1) a realistic density front between the subtropical and subpolar circulations and (2) a poleward shift of the center of the gyre with depth.

The ACC as Part of a Global Ocean Model

The ACC is really a part of the global ocean and should be modeled in that manner. Currently, it is not possible, because of computer limitations, to solve numerical models of the world ocean that have all of the dynamical processes, especially mesoscale, that are thought to be important in large-scale circulation. However, some models exist having approximations to these processes, and it is appropriate to assess how well they represent the ACC. Four models of varying complexity are considered.

The simplest model [Veronis, 1973] was a modified Sverdrup calculation for a two-layer world ocean forced by the climatological winds of Hellerman [1967]. The lower layer was motionless unless exposed to the wind (mainly in the polar regions). Because the Sverdrup solution allows no latitude lines within the flow to continue without meridional boundaries, the South Scotia Arc and the Antarctic Peninsula were assumed to block the ACC. The calculated transport through Drake Passage was more than $200 \times 10^6 \text{ m}^3/\text{s}$, and the structure of the flow in the southern ocean bore some resemblance to observations (Figure 13). In spite of the reasonably good estimate for the total transport, this model addresses the forced flow and not the higher order dynamics of the ACC, which may be especially important at Drake Passage. It does show the role of simple Sverdrup dynamics in the large scale circulation in the southern ocean.

Bryan and Cox [1972] described a nine-level, primitive equation world ocean model forced by the Hellerman [1967] winds. The water is assumed to be homogeneous even though the vertical structure of the flow is calculated. Separate polar, mid-latitude, and equatorial grids are used, and the solutions are patched together between these regions. The horizontal resolution is $2^\circ \times 2^\circ$, which gives a distance between grid points which is everywhere less than 220 km. Lateral friction is somewhat high, resulting in a Munk boundary layer 300 km wide, or 2 to 3 times too large. Solutions with and without bottom topography are presented. The model ACC has a transport of $32 \times 10^6 \text{ m}^3/\text{s}$ with realistic bottom topography.

These values do not compare well with the known transport in Drake Passage; stratification is assumed to provide the missing physics and thus improve the comparison.

In a following study, Cox [1975] considered the effect of stratification by calculating the circulation with the average temperature and salinity fields. In one calculation the stratification was fixed, and the transport at Drake Passage increased to $184 \times 10^6 \text{ m}^3/\text{s}$. A second calculation allowed the stratification to change in response to the circulation. The model was run for only 2.3 model years, which was insufficient for a steady state. This resulted in a slight increase of ACC transport to $186 \times 10^6 \text{ m}^3/\text{s}$.

Using a different primitive equation world ocean model, Bye and Sag [1972] considered vertically integrated circulation, with and without bottom topography, as forced by the Hellerman [1967] winds. Three different numerical grids were used, with horizontal resolutions between 2° and 5° . Viscous dissipation was provided by bottom friction alone. For the flat bottom simulation with realistic bottom friction, the ACC transport was about $340 \times 10^6 \text{ m}^3/\text{s}$; with realistic bottom topography the transport reduced to $15\text{--}20 \times 10^6 \text{ m}^3/\text{s}$ more or less independent of the choice of friction parameter. The inclusion of stratification was suggested as a means to increase the transport to a more realistic value.

A coupled ocean-atmosphere climate model [Bryan *et al.*, 1975] includes a stratified (12 level) ocean with both realistic coastline and bottom topography. The maximum horizontal grid spacing for the ocean is 700 km. A nonlinear equation of state is used to convert model temperature and salinity to density. The climatological steady state for the model ocean has reasonable flow patterns, but the current speeds are slower than observed. The ACC, in particular, has a transport of only $22 \times 10^6 \text{ m}^3/\text{s}$. The zonally averaged model surface winds in the southern hemisphere are weaker than observed surface winds, and the "Roaring 40's" are missing entirely, which may account for the low transport of the ACC.

Mesoscale Dynamics in the ACC

The studies mentioned thus far (except that of McWilliams and Chow [1981]) have taken a large-scale view of the dynamics of the ACC; that is, the length scales have been longer than several hundred kilometers. Mesoscale dynamics, occurring on scales of 10–200 km, need to be considered for possible importance in the southern ocean. Two general classes of mesoscale effects are reviewed here: flow-topography interaction and eddy-mean flow interaction. Both partial meridional barriers and bottom topography can produce flow perturbations with length scales equal to a few internal radii of deformation (say, 40–150 km). Such perturbations can enhance dissipation in the flow through the creation of mesoscale eddies.

Wind-driven flow in a basin with a partial meridional barrier (simulating Africa) was considered by de Ruijter [1982]. Special emphasis was placed on the dynamic processes that occur at the tip of the barrier, where the Agulhas Current leaves the continent and turns eastward (so-called "retroreflection"). Both linear and nonlinear models with lateral friction were used, in which the interior is in Sverdrup balance with the wind. Munk-type boundary layers develop on the western side of each gyre and around the tip of the partial barrier. A spreading, free viscous boundary layer allows water that flows around the partial barrier to move to the far western boundary of the ocean. In a linear calculation, all of the flow on the eastern coast of Africa rounds the tip and enters

the Atlantic Ocean. A nonlinear calculation shows that some of this water turns sharply eastward in the region south of Africa and flows back into the Indian Ocean. The structure of the wind curl over the ocean south of Africa determines the amount of water which moves westward and that which turns back eastward into the Indian Ocean. Therefore the model results are quite sensitive to the shape of the wind curl over this small region of the ocean.

Smith and Fandry [1978] use a two-layer model of a zonal channel to compare the effects of stratification and bottom topography (essentially a two-layer version of the Kamenkovich [1962] model). Vertical viscosity is incorporated by including surface, interface, and bottom Ekman layers; wind stress drives the circulation. The flow follows geostrophic contours (lines of constant f/depth) under the assumption that planetary beta is small compared to topographic beta. For flow along a ridge, they find that the speed is higher and a density front can develop on the equatorward side of the ridge. This effect may play some role in the formation of density fronts in the ACC.

McCartney [1976] examined eastward zonal flow of a stratified, rotating fluid over meridional and zonal ridges and over isolated seamounts. There is a natural length scale of $(u/\beta)^{1/2}$, where u is the mean speed and β is the gradient of the Coriolis parameter, associated with these flow interactions, implying that mesoscale flow patterns can be created from large-scale oceanic flow. In particular, a meridional ridge produces lee waves. A zonal ridge induces faster flow on the equatorward side of the ridge and, for finite length, a vortex street downstream of the ridge. An isolated seamount produces an anticyclonic meander on its upstream, equatorward side and a cyclonic meander on its downstream, poleward side. The intensity of these meanders increases with increasing height of the topography.

Boyer and Guala [1972] analyzed flow over the complex ridge and trench system south of New Zealand by using a one-layer numerical model and a laboratory model. The numerical model used f plane dynamics and was forced by un-sheared, eastward flow. Vertical friction ($A_v = 10^{-3} \text{ m}^2/\text{s}$) was used to damp the flow. The numerical model agreed quite well with the laboratory simulation. Neglecting beta effects, the flow disturbance is trapped to the topography (geostrophic contours are identical with topographic contours), and Rossby lee waves are not permitted. Given the large friction and the f plane assumption, the model cannot be compared easily with the observed oceanic currents in this region.

Mesoscale flow features are also created by barotropic and baroclinic instabilities. The resulting eddies interact with the mean flow to redistribute energy and vorticity both horizontally and vertically. The analysis of strongly interacting eddy flows requires the use of numerical models with horizontal resolution at least as small as the internal radius of deformation. Such models put considerable strain on present computer resources, so they are usually employed to demonstrate the dynamics in reduced domains rather than as complete replicas of a natural system.

McWilliams *et al.* [1978] described an eddy-resolving, two-layer, wind-forced numerical model of a zonal channel with partial meridional barriers. In this model the wind is zonal with a sinusoidal distribution that is zero at the northern and southern edges of the basin and maximum (eastward) in the center. Linear bottom friction and biharmonic lateral friction are specified in the model, but eddies, created by flow instabil-

minimum of instrumentation. A second transport measurement is needed south of Australia or New Zealand. Time correlations between these two transport series will begin to answer questions about the angular momentum of the ACC as a whole. There have been several estimates of the time lag of the ACC in response to changes in wind forcing. Such transport time series will help sort out the temporal behavior of the ACC and its relation to forcing. As a long-range goal, satellite altimetry coupled with sea level stations (including atmospheric surface pressure) and deep pressure observations, should be used to calculate the transport of the ACC at several places about the southern ocean, not just in the narrow parts of the current system.

Improved fields of atmosphere-ocean exchanges of momentum, heat and moisture are needed to improve our understanding of the circulation and heat budget of the southern ocean. Climatology for the southern ocean is hampered by its remoteness as well as its dependably bad weather. It seems that satellite observations (for example, the scatterometer on NROSS) offer the only hope for obtaining wind stress observations with adequate geographical coverage. Heat exchange with the atmosphere is an important element of water mass conversions which occur in many places in the southern ocean. Such heat flux estimates will be necessary for the development of thermodynamically active models of the ACC.

The correct dynamical balance for the ACC is still not known. The roles of continental boundaries, stratification, bottom topography, and dynamic instabilities have been shown to be important separately, but such effects have not been considered all in the same numerical model. As an example of the interrelation of these factors, the meridional distribution of wind forcing in relation to the meridional extent of land barriers has been shown to be of considerable importance. Finally, active thermodynamics should be included in these models to consider how newly formed, dense water is able to cross the ACC without losing its distinctive character.

The dynamics of the creation and maintenance of the ACC fronts and their associated strong currents should be investigated. Such currents seem to be sensitive to bottom topography and tend to flow through gaps in bathymetry. These deep-reaching currents are shown to be unstable in Drake Passage where they have been extensively investigated, and they may be unstable throughout the remainder of the ACC. The stability of these currents has an impact on the meridional exchange of heat, momentum, and other properties across the ACC. Investigations should include both theoretical and observational points of view.

Simple indices which give good indications of the behavior of the ACC, or some parts thereof, may exist. Specific observations in the surface meteorological fields, for example, surface winds, may signal variations in the current fields of the southern ocean. The ACC transport observations should be compared through the use of models with surface wind fields. Some surface wind fields are available now that are contemporaneous with transport observations in Drake Passage; the next decade promises improvements in observations of both wind stress and current variations.

Acknowledgment. This work was supported by the Ocean Sciences Division of the National Science Foundation.

REFERENCES

- Ad Hoc Working Group on Antarctic Oceanography, Southern ocean dynamics: A strategy for scientific exploration, 1973-1983, report, 52 pp., National Academy of Sciences, Washington, D. C., 1974.
- Allen, J. S., M. S. McCartney, and T. Yao, Topographically-induced jets in a zonal channel with application to the Drake Passage (abstract), *Eos Trans. AGU*, 56(12), 1011, 1975.
- Baker, D. J., Jr., A note on Sverdrup balance in the southern ocean, *J. Mar. Res.*, 40, suppl., 21-26, 1982.
- Baker, D. J., Jr., W. D. Nowlin, Jr., R. D. Pillsbury, and H. L. Bryden, Antarctic Circumpolar Current: Space and time fluctuations in the Drake Passage, *Nature*, 268(5622), 696-699, 1977.
- Barclon, V., On the influence of the peripheral antarctic water discharge on the dynamics of the circumpolar current, *J. Mar. Res.*, 24, 269-275, 1966.
- Barclon, V., Further investigation of the influence of the peripheral antarctic water discharge of the circumpolar current, *J. Mar. Res.*, 25, 1-9, 1967.
- Boyer, D. L., and J. R. Guala, Model of the Antarctic Circumpolar Current in the vicinity of the Macquarie Ridge, in *Antarctic Oceanology II, The Australian-New Zealand Sector*, *Antarct. Res. Ser.*, vol. 19, edited by D. E. Hayes, pp. 79-93, AGU, Washington, D. C., 1972.
- Bryan, K., and M. Cox, The circulation of the world ocean: A numerical study, I, A homogeneous model, *J. Phys. Oceanogr.*, 2, 319-335, 1972.
- Bryan, K., S. Manabe, and R. C. Pacanowski, A global ocean-atmosphere climate model, II, The oceanic circulation, *J. Phys. Oceanogr.*, 5, 30-46, 1975.
- Bryden, H. L., Poleward heat flux and conversion of available potential energy in Drake Passage, *J. Mar. Res.*, 37, 1-22, 1979.
- Bryden, H. L., The southern ocean, in *Eddies in Marine Science*, edited by A. R. Robinson, pp. 265-277, Springer, New York, 1983.
- Bryden, H. L., and R. A. Heath, Energetic eddies at the northern edge of the Antarctic Circumpolar Current in the southwest Pacific, *Prog. Oceanogr.*, 14, 65-87, 1985.
- Bryden, H. L., and R. D. Pillsbury, Variability of deep flow in the Drake Passage from year-long current measurements, *J. Phys. Oceanogr.*, 7, 803-810, 1977.
- Bye, J. A. T., and T. W. Sag, A numerical model for circulation in a homogeneous world ocean, *J. Phys. Oceanogr.*, 2, 305-318, 1972.
- Chelton, D. B., Statistical reliability and the seasonal cycle: Comments on "Bottom pressure measurements across the Antarctic Circumpolar Current and their relation to the wind," *Deep Sea Res., Part A*, 29(11), 1381-1388, 1982.
- Cheney, R. E., J. G. Marsh, and B. D. Beckley, Global mesoscale variability from collinear tracks of SEASAT altimetry data, *J. Geophys. Res.*, 88(C7), 4343-4354, 1983.
- Clarke, A. J., The dynamics of large-scale, wind-driven variations in the Antarctic Circumpolar Current, *J. Phys. Oceanogr.*, 12, 1092-1105, 1982.
- Clifford, M. A., A descriptive study of the zonation of the Antarctic Circumpolar Current and its relation to wind stress and ice cover, M.S. thesis, 93 pp., Tex. A&M Univ., College Station, 1983.
- Colton, M. T., and R. P. Chase, Interaction of the Antarctic Circumpolar Current with bottom topography: An investigation using satellite altimetry, *J. Geophys. Res.*, 88(C3), 1825-1843, 1983.
- Cox, M. D., A baroclinic numerical model of the world ocean: Preliminary results, in *Numerical Models of Ocean Circulation*, pp. 107-120, National Academy of Sciences, Washington, D. C., 1975.
- Deacon, G. E. R., The hydrology of the southern ocean, *Discovery Rep.*, 15, 3-122, 1937.
- Deacon, G. E. R., Physical and biological zonation in the Southern Ocean, *Deep Sea Res., Part A*, 29, 1-15, 1982.
- de Ruijter, W., Asymptotic analysis of the Agulhas and Brazil current systems, *J. Phys. Oceanogr.*, 12, 361-373, 1982.
- deSzoeko, R. A., and M. D. Levine, The advective flux of heat by mean geostrophic motions in the southern ocean, *Deep Sea Res.*, 28(10), 1057-1085, 1981.
- Devine, M., Some aspects of the dynamics of the Antarctic Circumpolar Current, *J. Geophys. Res.*, 77, 5987-5992, 1972.
- Emery, W. J., Antarctic Polar Frontal Zone from Australia to the Drake Passage, *J. Phys. Oceanogr.*, 7(6), 811-822, 1977.
- Fandry, C., Baroclinic instability of the Antarctic Circumpolar Current in the Drake Passage, *Ocean Modelling*, 22, May 8-9, 1979.
- Fandry, C., and R. D. Pillsbury, On the estimation of absolute geostrophic volume transport applied to the Antarctic Circumpolar Current, *J. Phys. Oceanogr.*, 9(3), 449-455, 1979.

- Fofonoff, N., A theoretical study of zonally uniform flow, Ph.D. dissertation, Brown Univ., Providence, R. I., 1955.
- Foster, L. A., Current measurements in the Drake Passage, M.S. thesis, 61 pp., Dalhousie Univ., Halifax, N. S., Canada, 1972.
- Fu, L.-L., and D. B. Chelton, Temporal variability of the Antarctic Circumpolar Current observed from satellite altimetry, *Science*, 226, 343–346, 1984.
- Garrett, J. F., Oceanographic features revealed by the FGGE drifting buoy array, in *Oceanography From Space*, edited by J. F. R. Gower, pp. 61–69, Plenum, New York, 1981.
- Georgi, D. T., and J. M. Toole, The Antarctic Circumpolar Current and the oceanic heat and freshwater budgets, *J. Mar. Res.*, 40, suppl., 183–197, 1982.
- Gill, A. E., A linear model of the Antarctic Circumpolar Current, *J. Fluid Mech.*, 32, 465–488, 1968.
- Gill, A. E., and K. Bryan, Effects of geometry on the circulation of a three-dimensional southern hemisphere ocean model, *Deep Sea Res.*, 18, 685–721, 1971.
- Gordon, A. L., Structure of Antarctic waters between 20°W and 170°W, *Antarct. Map Folio Ser.*, folio 6, edited by V. Bushnell, 10 pp., 14 plates, Am. Geogr. Soc., N.Y., 1967.
- Gordon, A. L., Seasonality of southern ocean sea ice, *J. Geophys. Res.*, 86(C5), 4193–4197, 1981.
- Gordon, A. L., and E. J. Molinelli, *Southern Ocean Atlas*, 11 pp., 233 plates, Columbia University Press, New York, 1982.
- Gordon, A. L., and H. W. Taylor, Heat and salt balance within the cold waters of the world ocean, in *Numerical Models of Ocean Circulation*, pp. 54–56, National Academy of Science, Washington, D. C., 1975.
- Gordon, A. L., H. W. Taylor, and D. T. Georgi, Antarctic oceanographic zonation, in *Polar Oceans, Proceedings of the Polar Oceans Conference*, edited by M. J. Dunbar, pp. 45–76, Arctic Institute of North America, Calgary, Alberta, Canada, 1977a.
- Gordon, A. L., D. T. Georgi, and H. W. Taylor, Antarctic Polar Front Zone in the western Scotia Sea—Summer 1975, *J. Phys. Oceanogr.*, 7(3), 309–328, 1977b.
- Gordon, A. L., E. Molinelli, and T. Baker, Large-scale relative dynamic topography of the southern ocean, *J. Geophys. Res.*, 83(C6), 3023–3032, 1978.
- Han, Y.-J., and S.-W. Lee, A new analysis of monthly mean wind stress over the global ocean, *Rep. 26*, 148 pp., Clim. Res. Inst., Oreg. State Univ., Corvallis, 1981.
- Hastenrath, S., On meridional heat transport in the world ocean, *J. Phys. Oceanogr.*, 12(8), 922–927, 1982.
- Haynes, P. H., Wind gyres in circumpolar oceans, *J. Phys. Oceanogr.*, 15, 670–683, 1985.
- Heath, R. A., Oceanic fronts around southern New Zealand, *Deep Sea Res., Part A*, 28A, 547–560, 1981.
- Hellerman, S., An updated estimate of the wind stress on the world ocean, *Mon. Weather Rev.*, 95, 607–626, 1967.
- Hidaka, K., and M. Tsuchiya, On the Antarctic Circumpolar Current, *J. Mar. Res.*, 12, 214–222, 1953.
- Hofmann, E. E., The large-scale horizontal structure of the Antarctic Circumpolar Current from FGGE drifters, *J. Geophys. Res.*, 90, 7087–7097, 1985.
- Hofmann, E. E., and T. Whitworth III, A synoptic description of the flow at Drake Passage from yearlong measurements, *J. Geophys. Res.*, 90, 7177–7187, 1985.
- Inoue, M., Vertical structure of the low-frequency currents at Drake Passage, Ph.D. dissertation, 220 pp., Tex. A&M Univ., College Station, 1982.
- Inoue, M., Modal decomposition of the low-frequency currents and baroclinic instability at Drake Passage, *J. Phys. Oceanogr.*, 15, 1157–1181, 1985.
- Jenne, R. L., H. I. Crutcher, H. van Loon, and J. J. Taljaard, Climate of the upper air southern hemisphere, III, Vector mean geostrophic winds: Isoaon and isotach analysis, *Rep. NCAR-TN/STR-58*, Natl. Center for Atmos. Res., Boulder, Colo., 1971.
- Johnson, J. A., and R. B. Hill, A three-dimensional model of the southern ocean with bottom topography, *Deep Sea Res.*, 22, 745–751, 1975.
- Joyce, T. M., A note on the lateral mixing of water masses, *J. Phys. Oceanogr.*, 7(4), 626–629, 1977.
- Joyce, T. M., and S. L. Patterson, Cyclonic ring formation at the polar front in the Drake Passage, *Nature*, 265(5590), 131–133, 1977.
- Joyce, T. M., W. Zenk, and J. M. Toole, The anatomy of the Antarctic Polar Front in the Drake Passage, *J. Geophys. Res.*, 83(C12), 6093–6113, 1978.
- Joyce, T. M., S. L. Patterson, and R. C. Millard, Anatomy of a cyclonic ring in the Drake Passage, *Deep Sea Res., Part A* 28(11), 1265–1287, 1981.
- Kamenkovich, V. M., Towards a theory of the Antarctic Circumpolar Current (in Russian), *Tr. Inst. Okeanol. im. P. P. Shirshova, Akad. Nauk SSSR*, 56, 1962.
- Klinck, J. M., EOF analysis of central Drake Passage currents from DRAKE 79, *J. Phys. Oceanogr.*, 15, 288–298, 1985.
- Legeckis, R., Oceanic polar front in the Drake Passage—Satellite observations during 1976, *Deep Sea Res.*, 24, 701–704, 1977.
- Lutjeharms, J. R. E., Location of frontal systems between Africa and Antarctica: Some preliminary results, *Deep Sea Res., Part A*, 32(12), 1499–1510, 1985.
- Lutjeharms, J. R. E., and D. J. Baker, Jr., A statistical analysis of the meso-scale dynamics of the southern ocean, *Deep Sea Res., Part A*, 27(2), 145–159, 1980.
- Mackintosh, N. A., The antarctic convergence and the distribution of surface temperature in Antarctic waters, *Discovery Rep.*, 23, 177–212, 1946.
- Meinardus, W., Ergebnisse der Seefahrt des Gauss, *Dtsch. Sudpol. Exped. 1901–1903*, 3, 531, 1923.
- McCartney, M. S., The interaction of zonal currents with topography with applications to the southern ocean, *Deep Sea Res.*, 23, 413–427, 1976.
- McCartney, M. S., Subantarctic Mode Water, in *A Voyage of Discovery*, edited by M. Angel, pp. 103–119, Pergamon, New York, 1977.
- McCartney, M. S., The subtropical recirculation of mode waters, *J. Mar. Res.*, 40, suppl., 427–464, 1982.
- McWilliams, J. C., and J. H. S. Chow, Equilibrium geostrophic turbulence, I, A reference solution in a beta-plane channel, *J. Phys. Oceanogr.*, 11, 921–949, 1981.
- McWilliams, J. C., W. R. Holland, and J. H. S. Chow, A description of numerical antarctic circumpolar currents, *Dyn. Atmos. Oceans*, 2, 213–291, 1978.
- Munk, W. H., and E. Plamén, Note on the dynamics of the Antarctic Circumpolar Current, *Tellus*, 3, 53–55, 1951.
- Nowlin, W. D., Jr., and M. Clifford, The kinematic and thermohaline zonation of the Antarctic Circumpolar Current at Drake Passage, *J. Mar. Res.*, 40, suppl., 481–507, 1982.
- Nowlin, W. D., Jr., T. Whitworth III, and R. D. Pillsbury, Structure and transport of the Antarctic Circumpolar Current at Drake Passage from short-term measurements, *J. Phys. Oceanogr.*, 7(6), 788–802, 1977.
- Nowlin, W. D., Jr., R. D. Pillsbury, and J. Bottero, Observations of kinetic energy levels in the Antarctic Circumpolar Current at Drake Passage, *Deep Sea Res.*, 28(1), 1–17, 1981.
- Nowlin, W. D., Jr., J. S. Bottero, and R. D. Pillsbury, Observations of principal tidal currents at Drake Passage, *J. Geophys. Res.*, 87(C7), 5752–5770, 1982.
- Nowlin, W. D., Jr., S. J. Worley, and T. Whitworth III, Methods for making point estimates of eddy heat flux as applied to the Antarctic Circumpolar Current, *J. Geophys. Res.*, 90(C2), 3305–3324, 1985.
- Nowlin, W. D., Jr., J. S. Bottero, and R. D. Pillsbury, Observations of internal and near-inertial oscillations at Drake Passage, *J. Phys. Oceanogr.*, 16(1), 87–108, 1986.
- Patterson, S. L., Surface circulation and kinetic energy distributions in the southern hemisphere oceans from FGGE drifting buoys, *J. Phys. Oceanogr.*, 15(7), 865–884, 1985.
- Peterson, R. G., W. D. Nowlin, Jr., and T. Whitworth III, Generation and evolution of a cyclonic ring at Drake Passage in early 1979, *J. Geophys. Res.*, 12(7), 712–719, 1982.
- Pillsbury, R. D., and J. S. Bottero, Observations of current rings in the Antarctic Zone at Drake Passage, *J. Mar. Res.*, 42, 853–874, 1984.
- Ratray, M., Jr., Time dependent motion in an ocean: A unified two-layer, beta-plane approximation, in *Studies on Oceanography*, edited by K. Yoshida, pp. 19–29, University of Tokyo Press, Japan., 1964.
- Reid, J. L., On the mid-depth circulation of the world ocean, in *Evolution of Physical Oceanography: Scientific Surveys in Honor of Henry Stommel*, edited by B. A. Warren and C. Wunsch, pp. 70–111, MIT Press, Cambridge, Mass., 1981.
- Reid, J. L., and W. D. Nowlin, Jr., Transport of water through the Drake Passage, *Deep Sea Res.*, 18, 51–64, 1971.
- Reid, R. O., B. A. Elliott, and D. B. Olson, Available potential energy: A clarification, *J. Phys. Oceanogr.*, 11, 15–29, 1981.
- Rojas, R. L., Eddy heat fluxes at Drake Passage due to mesoscale

- motions, M.S. thesis, 130 pp., Tex. A&M Univ., College Station, 1982.
- Sarukhanyan, E. I., *Structure and Variability of the Antarctic Circumpolar Current*, Amerind, New Delhi, 1985.
- Sarukhanyan, E. I., and N. P. Smirnov (Eds.), *Investigations of the POLEX SOUTH-78 Program*, Amerind, New Delhi, 1985.
- Savchenko, V. G., W. J. Emery, and O. A. Vladimirov, A cyclonic eddy in the Antarctic Circumpolar Current south of Australia; Results of Soviet-American observations aboard the R/V *Professor Zubov*, *J. Phys. Oceanogr.*, *8*, 825-837, 1978.
- Schulman, E. E., The Antarctic Circumpolar Current, paper presented at Summer Computer Simulation Conference, Natl. Sci. Found., Denver, Colo., June 1970.
- Sciremammano, F., Jr., Observations of Antarctic Polar Front motions in a deep water expression, *J. Phys. Oceanogr.*, *9*(1), 221-226, 1979.
- Sciremammano, F., Jr., The nature of the poleward heat flux due to low-frequency current fluctuations in Drake Passage, *J. Phys. Oceanogr.*, *10*, 843-852, 1980.
- Sciremammano, F., Jr., R. D. Pillsbury, W. D. Nowlin, Jr., and T. Whitworth III, Spatial scales of temperature and flow in Drake Passage, *J. Geophys. Res.*, *85*(C7), 4015-4028, 1980.
- Sievers, H. A., and W. D. Nowlin, Jr., The stratification and water masses in Drake Passage, *J. Geophys. Res.*, *83*, 10,489-10,514, 1984.
- Smith, N. R., and C. B. Fandry, Combined effects of wind stress and topography in a two-layer model of the southern ocean, *Deep Sea Res.*, *25*, 371-390, 1978.
- Stommel, H., A survey of ocean current theory, *Deep Sea Res.*, *4*, 149-184, 1957.
- Taylor, H. W., Some large-scale aspects of the southern ocean and its environment, Ph.D. thesis, Lamont-Doherty Geol. Observ., Columbia Univ., Palisades, N. Y., 1978.
- Taylor, H. W., A. L. Gordon, and E. Molinelli, Climate characteristics of the Antarctic Polar Front Zone, *J. Geophys. Res.*, *83*(C9), 4572-4578, 1978.
- Toole, J. M., Sea ice, winter convection, and the temperature minimum layer in the southern ocean, *J. Geophys. Res.*, *86*(C9), 8037-8047, 1981.
- Veronis, G., Model of world ocean circulation, I, Wind-driven, two-layer, *J. Mar. Res.*, *31*, 228-288, 1973.
- Wearn, R. B., Jr., and D. J. Baker, Jr., Bottom pressure measurements across the Antarctic Circumpolar Current and their relation to wind, *Deep Sea Res., Part A*, *27*(11), 875-888, 1980.
- Whitworth, T., III, Monitoring the transport of the Antarctic Circumpolar Current at Drake Passage, *J. Phys. Oceanogr.*, *13*, 2045-2057, 1983.
- Whitworth, T., III, and R. G. Peterson, The volume transport of the Antarctic Circumpolar Current from three-year bottom pressure measurements, *J. Phys. Oceanogr.*, *15*(6), 810-816, 1985.
- Whitworth, T., III, W. D. Nowlin, Jr., and S. J. Worley, The net transport of the Antarctic Circumpolar Current through Drake Passage, *J. Phys. Oceanogr.*, *12*, 960-971, 1982.
- Wright, D. G., Baroclinic instability in Drake Passage, *J. Phys. Oceanogr.*, *11*, 231-246, 1981.
- Wyrki, K., The Antarctic Circumpolar Current and the Antarctic Polar Front, *Dtsch. Hydrogr. Z.*, *3*, 153-173, 1960.
- Wyrki, K., L. Magaard, and J. Hager, Eddy energy in the oceans, *J. Geophys. Res.*, *81*(15), 2641-2646, 1976.
- Zillman, J. W., Solar radiation and sea-air interaction south of Australia, in *Antarctic Oceanology II, The Australian-New Zealand Sector, Antarct. Res. Ser.*, vol. 19, edited by D. E. Hayes, pp. 11-40, AGU, Washington, D. C., 1972.

J. M. Klinck and W. D. Nowlin, Jr., Department of Oceanography, Texas A&M University, College Station, TX 77843.

(Received January 9, 1986;
revised June 9, 1986;
accepted June 9, 1986.)